REPUBLIC OF TÜRKİYE
YILDIZ TECHNICAL UNIVERSITY
GRADUATE SCHOOL OF SCIENCE AND ENGINEERING

DEVELOPMENT OF GREEN WAVE CONTROL STRATEGY FOR OPTIMAL ENERGY CONSUMPTION IN ELECTRIC VEHICLES

Furkan ÖZKAN

MASTER OF SCIENCE

Department of Mechatronics Engineering

Program of Mechatronics Engineering

Supervisor

Assist. Prof. Hatice MERCAN

Co-Supervisor

Assoc. Prof. Mehmet Selçuk ARSLAN

Nov, 2024

REPUBLIC OF TÜRKİYE

YILDIZ TECHNICAL UNIVERSITY

GRADUATE SCHOOL OF SCIENCE AND ENGINEERING

DEVELOPMENT OF GREEN WAVE CONTROL STRATEGY FOR OPTIMAL ENERGY CONSUMPTION IN ELECTRIC VEHICLES

A thesis submitted by Furkan ÖZKAN in partial fulfillment of the requirements for the degree of **MASTER OF SCIENCE** is approved by the committee on 22.11.2024 in Department of Mechatronics, Program of Mechatronics Engineering.

Assist. Prof Hatice MERCAN Yıldız Technical University Supervisor	Assoc. Prof. Mehmet Selçuk ARSLAN Yıldız Technical University Co- supervisor

Approved By the Examining Committee

Assist. Prof. Hatice MERCAN, Supervisor
Yildiz Technical University _____

Assoc. Prof. Muhammet GARİP, Member
Yildiz Technical University _____

Prof. Dr. Volkan SEZER, Member
Istanbul Technical University _____

I hereby declare that I have obtained the required legal permissions during data collection and exploitation procedures, that I have made the in-text citations and cited the references properly, that I haven't falsified and/or fabricated research data and results of the study and that I have abided by the principles of the scientific research and ethics during my Thesis Study under the title of "Development of Green Wave Control Strategy for Optimal Energy Consumption in Electric Vehicles" supervised by my supervisor, Assist. Prof. Hatice MERCAN. In the case of a discovery of false statement, I am to acknowledge any legal consequence.

Furkan ÖZKAN

Signature

Dedicated to my wife

and my daughter

ACKNOWLEDGEMENTS

I would like to express my deepest gratitude to my advisors, Assist. Prof. Hatice MERCAN and especially co-advisor Assoc. Prof. Mehmet Selçuk ARSLAN for their unlimited patience, invaluable guidance, mentorship, and encouragement throughout the development of this thesis. Their insights and expertise have been instrumental in shaping the direction of my research. I am also grateful to my committee members for their constructive feedback and support.

I extend my thanks to AVL Turkey Research and Engineering for providing the resources and funding that made this research possible.

Finally, I would like to thank my wife and my family for their unwavering support, patience, and belief in me throughout this journey. Their encouragement gave me the strength to persevere during challenging times.

Furkan ÖZKAN

TABLE OF CONTENTS

LIST OF SYMBOLS

m	Vehicle Mass
Te	Vehicle's Engine Torque
η	Transmission Efficiency
N	Total Gear Ratio
Rwh	Wheel Radius
α	Road Grade
$r0$	Coefficients for a Specific Set of Tires
ρ	Air Density
Af	Frontal Area
Cd	Air Drag Coefficient
F	Force
V	Velocity
β	body slip angle
γ	Yaw Rate
Cf	Front Cornering Stiffnesses
Cr	Rear Cornering Stiffnesses
lf	Front Distance from the Center of Gravity
lr	Rear Distance from the Center of Gravity
M	Direct Yaw Moment
P_{ego}	Ego Vehicle's Position at Current Time Step
P_{pre}	Predicted Vehicle Position
d_{min}	Allowed Distance Between the Ego and Preceding Car
T_{st}	Driving Torque Required for Straight Running
X_{Veh}	Position of the Vehicle
X_{TLn}	Position of Traffic Light n

LIST OF ABBREVIATIONS

ECU	Electronic Control Unit
FNN	Feedforward-Neural-Network
FTP-75	Federal Test Procedure
GWCS	Green Wave Control System
IDM	Intelligent Driver Model
MPC	Model Predictive Control
PCC	Predictive Cruise Control
PSO	Particle Swarm Optimization
PWM	Pulse Width Modulation
V2I	Vehicle-to-Infrastructure
V2V	Vehicle-to-Vehicle
V2X	Vehicle-to-Everything

LIST OF FIGURES

LIST OF TABLES

ABSTRACT

DEVELOPMENT OF GREEN WAVE CONTROL STRATEGY FOR OPTIMAL ENERGY CONSUMPTION IN ELECTRIC VEHICLES

Furkan Özkan

Department of Mechatronics Engineering

Program of Mechatronics Engineering

Master of Science Thesis

Supervisor: Assist. Prof. Hatice Mercan

Co- supervisor: Assoc. Prof. Mehmet Selçuk Arslan

Electric vehicles are gaining popularity as a sustainable substitute for conventional combustion engine automobiles. Efficient control systems are crucial for fully harnessing the promise of electric vehicles (EVs) in minimizing environmental impact and energy usage. This study investigates the implementation of green wave control for electric cars through the use of model predictive control. Green wave control aims to optimize traffic light timing, allowing vehicles to travel smoothly through multiple intersections without stopping, thereby reducing energy consumption and emissions. Additionally, it incorporates energy consumption modeling by utilizing neural networks. Employing model predictive control (MPC) enables the cars to optimize their energy use in real-time, taking into account the changing traffic circumstances. By using neural networks to simulate energy usage, the performance of electric vehicles may be improved by making precise forecasts and implementing adaptive control. The use of these sophisticated control and modeling methods seeks to optimize energy economy and distance coverage when maneuvering through urban traffic situations.

The research findings provide useful insights into the possibilities of using green wave control to optimize energy usage for electric cars. The study also highlights the need of MPC and neural network modeling in this optimization process. This thesis study makes a valuable contribution to the progress of sustainable transportation systems and the broad acceptance of electric cars. In order to assess the efficiency of the green wave management approach in actual urban settings, thorough simulations were carried out utilizing a sophisticated vehicle model and authentic traffic conditions. The findings demonstrate that the combination of model predictive control and energy consumption modeling with neural networks has a substantial influence on the energy efficiency and driving distance of electric cars. By employing MPC, the electric vehicle dynamically adjusted its speed and acceleration pattern in real-time to maximize energy efficiency while still meeting journey time goals. The utilization of a neural network for energy consumption modeling yielded precise forecasts, allowing the vehicle to anticipate and adapt to fluctuations in traffic patterns. This, in turn, improved energy efficiency and extended the vehicle's range. In addition, the study found that implementing the green wave control method resulted in a decrease in energy usage and enhanced the overall driving experience by eliminating sudden changes in speed, resulting in a more seamless and pleasant journey for passengers. The results indicate that green wave control has the potential to significantly transform urban transportation by improving the energy consumption performance of electric cars and contributing to a more sustainable and efficient mobility environment.

Keywords: Electric Vehicles, Energy efficiency, Green Wave Control, Model Predictive Control, Neural Networks.

ÖZET

ELEKTRİKLİ ARAÇLARDA OPTİMAL ENERJİ TÜKETİMİ İÇİN YEŞİL DALGA KONTROL STRATEJİSİ GELİŞTİRİLMESİ

Furkan Özkan

Mekatronik Mühendisliği Anabilim Dalı

Mekatronik Mühendisliği

Yüksek Lisans Tezi

Danışman: DR. ÖĞR. ÜYESİ HATİCE MERCAN

Eş-Danışman: DOÇ.DR. MEHMET SELÇUK ARSLAN

Elektrikli araçlar (EV'ler), geleneksel içten yanmalı motorlu araçlara sürdürülebilir bir alternatif olarak popülerlik kazanmaktadır. Elektrikli araçların çevresel etkilerini en aza indirmek ve enerji kullanımını optimize etmek için verimli kontrol sistemleri gereklidir. Bu çalışma, elektrikli araçlar için model öngörülü kontrol (MPC) kullanarak yeşil dalga kontrolünün uygulanmasını araştırmaktadır. Ayrıca, enerji tüketimi modellemesini nöral ağlar kullanarak gerçekleştirmektedir. MPC kullanımı, araçların değişen trafik koşullarını dikkate alarak enerji kullanımını gerçek zamanlı olarak optimize etmelerini sağlar. Nöral ağlar kullanarak enerji tüketimini simüle etmek, doğru tahminler yaparak ve uyarlanabilir kontrol uygulayarak elektrikli araçların performansını artırabilir. Bu sofistike kontrol ve modelleme yöntemlerinin kullanımı, kentsel trafik durumlarında enerji ekonomisini ve menzil kapsamını optimize etmeyi amaçlar. Araştırma bulguları, elektrikli araçlar için enerji kullanımını optimize etmek amacıyla yeşil dalga kontrolünün kullanılma potansiyeli hakkında değerli bilgiler sunmaktadır. Çalışma ayrıca, bu optimizasyon sürecinde model öngörülü kontrol ve nöral ağ modellemesinin entegrasyonunun önemini vurgular. Bu çalışma, sürdürülebilir ulaşım sistemlerinin

ilerlemesine ve elektrikli araçların geniş kabul görmesine önemli bir katkı sağlar. Yeşil dalga yönetimi yaklaşımının gerçek kentsel ortamlardaki etkinliğini değerlendirmek için, sofistike bir araç modeli ve gerçek trafik koşulları kullanılarak kapsamlı simülasyonlar gerçekleştirilmiştir. Bulgular, model öngörülü kontrol ve nöral ağlarla enerji tüketimi modellemesinin kombinasyonunun elektrikli araçların enerji verimliliği ve sürüş mesafesi üzerinde önemli bir etkisi olduğunu göstermektedir. MPC kullanarak, elektrikli araç, yolculuk süresi hedeflerini karşılarken enerji verimliliğini maksimize etmek için hız ve ivme desenini gerçek zamanlı olarak dinamik bir şekilde ayarlamıştır. Enerji tüketimi modellemesi için nöral ağ kullanımı, aracın trafik kalıplarındaki dalgalanmaları öngörüp uyum sağlamasına olanak tanıyan kesin tahminler sağladı. Bu da enerji verimliliğini artırmış ve aracın menzilini uzatmıştır. Ayrıca, çalışma yeşil dalga kontrol yönteminin uygulanmasının enerji kullanımında azalmaya ve ani hız değişikliklerinin ortadan kaldırılmasıyla genel sürüş deneyiminin iyileşmesine yol açtığını, böylece yolcular için daha sorunsuz ve keyifli bir yolculuk sağladığını bulmuştur. Sonuçlar, yeşil dalga kontrolünün kentsel ulaşımı önemli ölçüde dönüştürme potansiyeline sahip olduğunu, elektrikli araçların performansını artırarak daha sürdürülebilir ve verimli bir hareketlilik ortamına katkıda bulunduğunu göstermektedir.

Anahtar Kelimeler: Elektrikli araçlar, Enerji verimliliği, Yeşil dalga kontrolü, Model öngörülü kontrol, Sinir ağları.

1
INTRODUCTION

1.1 Background and Motivation

In recent years, electric vehicles have gained significant attention due to their potential in reducing CO_2 emissions and decreasing dependence on fossil fuels in the transportation sector. However, one of the challenges faced by electric vehicles is the limited range and the need for charging infrastructure. Electric vehicle development is being actively pursued by many countries, with various policies and incentives in place to promote their adoption. As a countermeasure to these challenges, the concept of "Green Wave" control strategy has emerged. Green Wave refers to a coordinated signal control strategy that aims to minimize energy consumption and improve traffic flow by synchronizing the timing of traffic signals along a specific route to allow a continuous flow of vehicles. Several studies have shown that implementing Green Wave control strategies can significantly reduce energy consumption and travel time for electric vehicles. The development of a Green Wave control strategy for electric vehicles involves the integration of advanced traffic signal control systems and vehicle-to-infrastructure communication technologies. By utilizing real-time traffic data and vehicle information, the Green Wave system can optimize the timing of traffic signals to create a "wave" of green lights for electric vehicles, minimizing the need for frequent accelerations and decelerations, thus improving energy efficiency.

Research in this area has focused on the design and implementation of algorithms that consider factors such as traffic flow, vehicle speed profiles, and energy consumption models to determine the optimal signal timing for achieving the Green Wave effect. Additionally, the use of predictive analytics and machine learning techniques has been explored to enhance the adaptability of the system to varying traffic conditions and to anticipate the energy demands of electric vehicles along the route.

As the adoption of electric vehicles continues to rise, the development of Green Wave control strategies presents a promising approach to address the challenges related to energy consumption and range limitations, ultimately contributing to the

sustainable and efficient integration of electric vehicles into the transportation ecosystem. The potential impact of Green Wave control strategies extends beyond the realm of electric vehicles, as it also holds promise for improving overall traffic flow and reducing energy consumption for all vehicles. As such, ongoing research and development efforts are crucial for refining the Green Wave concept and expanding its applicability across different transportation systems.

1.2 V2V & V2I Communication

Vehicle-to-vehicle (V2V) and vehicle-to-infrastructure (V2I) technologies play a crucial role in the successful implementation of Green Wave control strategies. These communication systems enable vehicles to exchange real-time data with one another and with infrastructure such as traffic signals and control centers, facilitating seamless coordination for optimizing traffic flow and energy efficiency. [1] [2]

In the context of Green Wave control, V2V communication allows vehicles within the green wave corridor to communicate and adjust their speed to maintain the optimal spacing for maximizing the efficiency of traffic signal synchronization. This capability enables not only reducing energy consumption and emissions but also promoting smoother traffic flow, benefiting both electric and conventional vehicles traversing the green wave route.

Furthermore, V2I communication empowers vehicles to interact with traffic signal systems and infrastructure, providing them with valuable information about signal timings and facilitating their integration into the green wave corridor. By receiving real-time data from traffic signals, vehicles can anticipate signal changes, adjust their speed, and minimize unnecessary accelerations and decelerations, thus contributing to overall energy efficiency and reduced emissions.

1.3 Green Wave

The implementation of Green Wave control strategies entails the coordination and synchronization of traffic signals along specific corridors to create a continuous flow of traffic with minimal stops. This approach aims to optimize energy

efficiency and reduce emissions, particularly for electric vehicles, by minimizing unnecessary accelerations and decelerations.

One of the key components of Green Wave implementation is the use of advanced traffic signal control systems that can adjust signal timings based on real-time traffic conditions. These systems utilize data from various sources, including V2V and V2I communication, to dynamically adapt signal patterns and maintain the green wave corridor.

Furthermore, the integration of Green Wave control with smart city initiatives involves leveraging data analytics and predictive modeling to anticipate traffic patterns and optimize signal timings proactively. By incorporating machine learning and artificial intelligence, traffic signal control systems can continuously adapt and evolve to ensure the efficient operation of the green wave corridor.

In addition to technological advancements, effective collaboration with city planners, traffic engineers, and environmental agencies is critical for the successful implementation of Green Wave control strategies. Local expertise and insights are invaluable for identifying the most suitable corridors for green wave deployment and addressing specific urban mobility challenges.

1.4 Objectives of the Thesis

The primary objective of this thesis is to develop a strategy to lower energy consumption in EVs by addressing one of the most energy-consuming actions: stop-and-go behavior at traffic lights. By implementing optimization algorithm which aims to optimize vehicle speed or acceleration to align the vehicle with green light timings where would reduces the unnecessary stop-and-gos.

This thesis focuses on developing longitudinal and lateral controllers for EVs. The longitudinal controller is MPC designed to avoid collisions and regulate speed and acceleration setpoints by its predictive capabilities. The lateral controller utilizes a Proportional-Integral-Derivative (PID) for smooth lane changes guided by Bézier curve. Lane change rules are integrated to enable changes when a slower vehicle is ahead to avoid changing the longitudinal setpoints unnecessarily. An energy consumption model, based on a neural network trained with real-time data, is developed to provide accurate predictions of energy usage. For optimal speed and

acceleration profiles, an algorithm which uses dynamic programming to calculate the setpoints based on the traffic light location, traffic light's green phase timing, vehicle location and vehicle speed is constructed. To compare the effectiveness of the control system an Intelligent Driver Model (IDM) implemented to benchmark energy consumption under various scenarios. The complete control system is tested in different conditions, and the optimization algorithm is integrated into an Electronic Control Unit (ECU) to validate its applicability in real-world driving environments.

1.5 Scope of Thesis

The scope of this thesis is confined to the development, implementation, and testing of an energy-efficient control system for EVs in city-to-city highway scenarios. The testing environment is designed to emulate real-world highway conditions with three lanes, based on the Federal Test Procedure (FTP-75) driving cycle. All the vehicles in the simulation operates within a speed range of 0 to 90 km/h, representing typical highway conditions, including stop-and-go traffic. For comfortable acceleration and deceleration limits of 3 m/s^2 and -2 m/s^2, respectively.

The control system is assumed to utilize V2V and V2I communication technologies to access real-time data. This includes the positions and green phase timings of traffic lights, as well as the positions and speeds of other vehicles in traffic. Such data enables the longitudinal controller to optimize speed and acceleration for energy efficiency while ensuring collision avoidance. Also, the lateral controller manages smooth lane changes based on traffic conditions, particularly for overtaking slower vehicles or maintaining flow, guided by lane change rules.

1.6 Thesis Organization

The structure of this thesis is outlined as follows:

Chapter 2 provides a literature review of Green Wave Technology, discussing its importance in reducing congestion, lowering emissions, and improving traffic flow. The chapter also addresses key barriers to the adoption of Green Wave systems, including technological, infrastructural, and behavioral challenges.

In Chapter 3, the vehicle models and energy estimation techniques used in this study are presented. A simplified lateral vehicle model, based on a two-wheel approach, supports longitudinal control, and energy consumption is estimated through a neural network. Bézier curves serve as set points for lateral control using a PID controller, while longitudinal control employs MPC to determine optimal speed and acceleration profiles.

Chapter 4 introduces the FTP-75 test to create realistic traffic scenarios for evaluating the Green Wave control system. Green wave optimization algorithm which includes the dynamics programing is introduced this chapter as well. The algorithm is also explained with an example calculation.

Chapter 5 presents the results of simulations, analyzing the green wave control system's effects on performance, energy consumption, and traffic efficiency. An IDM provides a basis for comparison, while five scenarios are designed to test collision avoidance and lane change mechanisms under various conditions The effectiveness of the collision avoidance and lane change algorithms is validated. The optimization algorithm is also integrated in to an ECU to validate the real-time applicability.

Finally, Chapter 6 concludes the thesis study by summarizing the main findings and proposing future research directions. This includes refining control algorithms, expanding simulation cases, and investigating new vehicle technologies to further improve the efficiency of green wave systems.

2
LITERATURE REVIEW

2.1 Overview of Electric Vehicles and their Energy Efficiency Challenges

The transition to electric vehicles is a crucial step towards a more sustainable transportation system, as it offers the potential to significantly reduce greenhouse gas emissions and air pollution [4]. However, the energy consumption of electric vehicles can be influenced by various driving regimes, and understanding these impacts is essential for optimizing the efficiency and environmental benefits of e-mobility [5] [6].

Recent studies have examined the factors that influence the adoption of electric vehicles, highlighting the importance of policies, consumer awareness, and technological advancements [7].

For instance, a study analyzing the electric vehicle adoption trends across the United States found that stringent emissions regulations and rising fuel prices are key drivers for increased EV adoption [7]. Another study that explored the social acceptance and user preferences of EVs identified the main obstacles as driving limitations, charging infrastructure, and consumer willingness-to-pay [8].

The energy consumption of electric vehicles can vary significantly depending on the driving regime, such as highway driving, urban driving, or a combination of both. Factors like vehicle speed, acceleration, and regenerative braking can all impact the energy efficiency of EVs.

A primary challenge of EVs is their support on energy-efficient operation across various driving conditions. Rapid acceleration and deceleration create significant energy demands on batteries, affecting both range and overall efficiency. To address this, it is essential to develop and optimize driving regimes, enabling energy-saving which would battery drain in high-demand driving scenarios.

The energy consumption of electric vehicles is a complex issue, as it depends on various factors, including the driving regime, vehicle characteristics, and the source of the electricity used to charge the batteries.

2.2 Literature Review

In the literature, there is limited research directly combining GWCS and MPC for optimal energy consumption in EVs. One recent research investigates an MPC-based car-following strategy for EVs, demonstrating improved energy efficiency compared to traditional methods [9]. Another similar study proposes a new system for autonomous vehicles that uses car-to-infrastructure communication to adjust their speed along a route. This helps them catch green lights, reducing stops, improving traffic flow by 30% and reducing energy use and pollution by nearly half. It works without changing traffic lights and could be used in current driver assistance systems and future self-driving cars [10]. The study in [11] proposes a new route planning method for EVs that considers both travel time and battery usage. They use traffic light data (green wave) and an ant colony optimization algorithm to find routes that balance these competing goals. Simulations show this method finds routes that are efficient and timely. A system for EVs that uses traffic signal info and V2I communication to recommend an energy-saving speed for catching green waves and minimizing fuel consumption was proposed in [12]. The system was tested through simulations. Another study proposes a new energy consumption model for electric vehicles [13]. With the increase in the number of vehicles on the road, traffic congestion, to address this issue, the authors propose a model that uses traffic signal control theory to design green wave scenarios, which can improve energy efficiency for electric vehicles.

The study in [14] presents a signal control method for urban road traffic using MPC to adjust traffic signals' parameters in real time. The method focuses on online adjustments of cycle times and offsets simultaneously. The paper introduces a simple model of small traffic with nonlinear dynamics and binary representation for green and red signals, which is then integrated into a mixed logical dynamical system. The researchers in [15] make a green light improved speed setpoint program and test how well it works by simulating three penetration rates. Results show that even vehicles that don't affected by the system directly gain efficiency when the penetration rate is high (70%). Some studies look at traffic data from a wider range and focuses on using information from a lot of different sources. In [16], the authors suggest a method for making a traffic map using ad-hoc contact

between vehicles. This would give drivers information about the speed of traffic in each lane. The Traffic Map is made from update of other V2V cars and their speeds.

The authors in [17] proposes the concept of predictive cruise control for the vehicles to optimize the fuel consumption and trip time, by using next traffic signal timing and phase information. A velocity trajectory planner is created for a subset of vehicles which is using short range radar and traffic signal information to generate the optimal velocity trajectory. Paper analyses the implementation of the Green-Wave Traffic theory using the two-phase signal control concept for cross intersections and T-intersections. It shows the benefits of the optimized Green-Wave traffic theory, for improving road safety, reducing vehicle fuel consumption, and decreasing vehicle emissions [18]. The optimization considers factors such as vehicle arrival characteristics, traffic organization, intersection spacing, and signal phase setting conditions. The researchers in [19] investigated the use of satellite positioning and network communication technology to increase effectiveness of green wave control by using floating vehicle trajectory data. The work in [20] presents a method for improving fuel economy using traffic data and a model predictive controller. It discusses how a vehicle can react to changes in traffic density or speed by using knowledge of the traffic ahead. This will increase trip efficiency and provides information to the driver. The paper mentions the utilization of traffic information to calculate a time-dependent velocity profile for the vehicle based on velocity constraints.

The research in [21] proposes a Predictive Cruise Control (PCC) to reduce fuel consumption and trip time in vehicle. This is done by using upcoming traffic signal timing and phase information. The objectives of research include arrival at green lights on timely manner, minimal braking, maintaining a safe distance between vehicles. The simulation results show significant fuel consumption reduction. The proposed concept different from current adaptive cruise control systems. The system minimizes braking, considers stop-and-go traffic, and receives timing signals from upcoming traffic lights. The paper shows the potential benefits of PCC for reducing traffic congestion and fuel consumption.

In [22], a bidirectional green-wave control method is proposed to help reduce urban traffic congestion and improve traffic flow. This method uses a random optimal graphical approach to allocate green-wave bandwidth based on road capacity in

both directions. It also introduces a formula for the bandwidth proration coefficient. The effectiveness of this method is tested using VISSIM simulation software and compared to the traditional graphical method. The paper includes a bidirectional green-wave band diagram. Simulation results show that this approach improves the capacity of optimized roads better than the traditional method.

In [23], a Multi-Intersection Coordination Algorithm is introduced to improve traffic flow and signal control using Vehicle-to-Everything (V2X) technology. The algorithm uses real-time traffic data from vehicle communication to create a signal strategy for multiple intersections. Simulations conducted with SUMO and MATLAB showed that the algorithm improves traffic capacity, reduces stops, and increases the average speed of vehicles on the roads.

Efficient energy management in EVs is crucial for sustainable transportation. Researchers show that using traffic management strategies such as; green-wave synchronization, bidirectional control, and intersection coordination by using V2I and V2V communication, potential for reducing energy consumption and emissions. However, most existing studies focus on a fixed number of traffic lights rather than considering all the lights along an entire route [14][15][18][23].

MPC is commonly used to predict and control vehicle speed or acceleration, to optimize fuel or energy consumption based on current traffic conditions. By adjusting the constraints of MPC, algorithms such as: collision-avoiding, car-following algorithms is possible, ensuring safe and efficient vehicle movement.

3
VEHICLE MODELS AND CONTROLLERS

3.1 Vehicle Models

In the development of modern autonomous vehicles, accurate modeling of vehicle dynamics is essential for ensuring both safety and efficiency. This chapter provides an introduction to three critical models used in the context of autonomous driving: The Longitudinal Dynamics Model, the Lateral Vehicle Model, and the Energy Consumption Model. Each of these models plays a vital role in simulating and controlling vehicle behavior.

For the Longitudinal Dynamic Model, Lateral Vehicle Model and their corresponding controllers following assumptions are made:

- Roads are assumed as asphalt.
- Roads have no grade.
- Vehicle is electric vehicle so that the engine characteristics are done by 2D Maps.
- Vehicles do not change speed while changing the lanes.

3.1.1 Longitudinal Vehicle Dynamics Model

The longitudinal dynamic model focuses on the forces and motions along the vehicle's direction of travel. It considers the vehicle's acceleration and deceleration influenced by factors such as applied torque, gear ratios, and external resistances like road grade and friction. For simplicity and robustness in our simulations, we assume constant parameters for gear ratio, road grade, road friction, and air density. This assumption allows the model to accurately predict vehicle speed and acceleration dynamics under various driving conditions without requiring real-time adjustments for these factors. The output of this model primarily governs the vehicle's forward motion, making it crucial for scenarios.

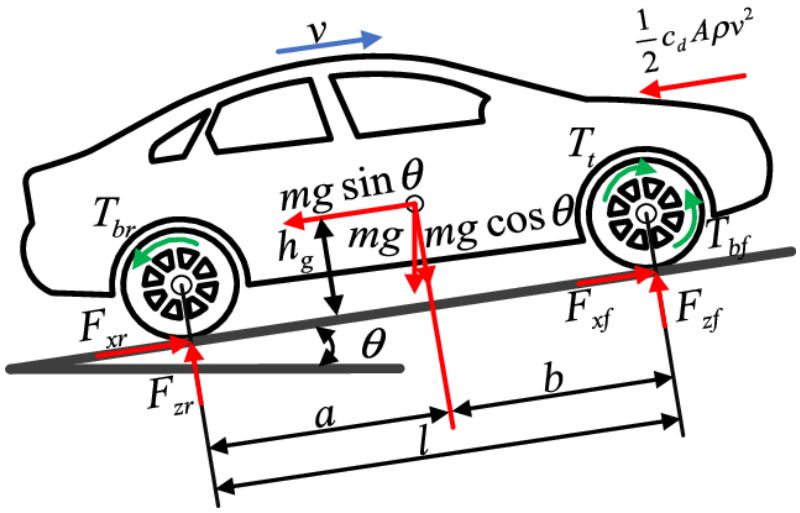

Figure 3.1 Longitudinal Dynamics Acting Forces

The vehicle's longitudinal dynamics is described by the following forces acting on the vehicle: The traction, road friction, aerodynamic resistance, road grade, and brake forces, (3.1)-(3.5) [25].

$$m\frac{dV}{dt} = F_{Trac} - F_{Roll} - F_{Aero} - F_{Grade} - F_{brake} \tag{3.1}$$

$$F_{Trac} = \frac{\eta N}{R_{wh}}.T_e \tag{3.2}$$

$$F_{Roll} = mg\cos(\alpha).(r_0 + r_1 V) \tag{3.3}$$

$$F_{Aero} = \frac{1}{2}\rho A_f C_d V^2 \tag{3.4}$$

$$F_{grade} = mg\sin(\alpha) \tag{3.5}$$

In the equations, m represents vehicle mass, T_e signifies engine torque, η indicates transmission efficiency, N refers the total gear ratio, R_{wh} denotes wheel radius, α represents the road grade, r_0 and r_1 are the coefficients which are calculated for specific tyres and surface of the road, ρ represents air density, A_f is the frontal area, C_d shown as the air drag coefficient, and F_{brake} is the brake force. Parameters of vehicle can be found in Appendix A.1.

Rearranging the above longitudinal dynamics equation (3) with the following assumptions:

- α is assumed as 0.
- EV has a constant gear,

we arrive at

$$\dot{v} = \frac{1}{C_1}(C_2 T_e - C_3{}^* V + C_4{}^* - F_{brake}) \tag{3.6}$$

where:

$$C_1 = \frac{1}{m} \tag{3.7}$$

$$C_2 = \frac{\eta \mathrm{N}}{R_{wh}} \tag{3.8}$$

$$C_3 = \tfrac{1}{2}\rho A_f C_d \tag{3.9}$$

$$C_4 = mg\cos(\alpha)\, r_0 \tag{3.10}$$

$$C_3{}^* = 2C_3 V \tag{3.11}$$

$$C_4{}^* = 2C_3 V^2 + C_4 \tag{3.12}$$

3.1.2 Lateral Vehicle Dynamics Model

The Lateral Vehicle Model is essential for understanding and controlling the side-to-side dynamics of a vehicle, particularly during lane-changing maneuvers. We employ a two-wheel planar vehicle model, which simplifies the vehicle to a bicycle-like representation with only two wheels in the plane of motion. This model is particularly suitable for our purposes because it integrates seamlessly with the longitudinal dynamics model; both models take the torque applied to the wheels as input, ensuring consistent and coordinated control of the vehicle's movement.

During lane-changing scenarios, we make a critical assumption that the vehicle's speed remains constant. This simplification allows us to focus solely on the lateral forces and the resulting trajectory of the vehicle, facilitating more straightforward calculations and control algorithms. By neglecting the speed decrease, the model can efficiently simulate lane changes, providing a foundation for developing advanced lane-changing algorithms that ensure smooth and safe transitions between lanes.

This study uses a two-wheel vehicle model, [26] and [27], to represent lateral and yaw motion dynamics. The vehicle planar model with a schematic diagram is shown in Figure 3.2.

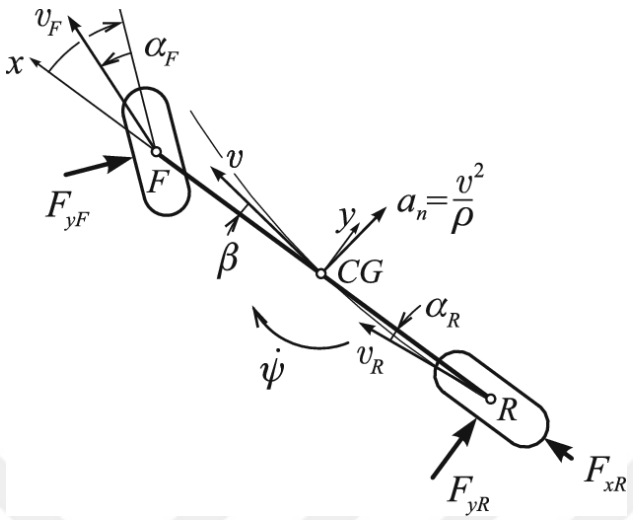

Figure 3.2 Two Wheel Vehicle Model Acting Forces

The equations governing the lateral and yaw motions of the vehicle is expressed in (3.13) and (3.14), respectively

$$mV(\dot{\beta}+\gamma) = 2C_f(\delta_f - l_f V\gamma\beta) + 2C_r(l_f V\gamma - \beta) \tag{3.13}$$

$$I\dot{\gamma} = 2l_f C_f(\delta_f - l_f\, V\gamma - \beta) - 2l_r C_r(l_r V\gamma - \beta) + M \tag{3.14}$$

where m denotes vehicle mass, I the yaw moment of inertia, velocity of the vehicle as V, β the body slip angle, $\gamma = \dot{\psi}$ the yaw rate, front and rear cornering stiffnesses as Cf and Cr, lf and lr front and rear distance from center to front and rear axle and M the direct yaw moment. Parameters of vehicle can be found in Appendix A.1.

3.1.3 Energy Consumption Estimation Model

Energy efficiency is a key concern in autonomous vehicle operation, making the Energy Consumption Model an indispensable component of our system. This model leverages Feedforward-Neural-Network (FNN) trained on real-world test data to predict the vehicle's energy consumption accurately. The neural network considers current vehicle speed and acceleration as inputs, enabling it to dynamically estimate energy usage under various driving conditions.

By using an FNN, we can encapsulate the complex interactions between vehicle dynamics, frictional forces, and battery characteristics in a black-box model. This approach allows for sophisticated energy consumption predictions without explicitly modeling every underlying physical process. The neural network's ability to learn from empirical data ensures that our energy consumption estimates remain accurate and reliable, even as driving conditions and vehicle states change.

In order to model energy consumption of an electrified vehicle based on the test data of a vehicle, which is provided by AVL, and user-defined parameters, a neural network was used. There are several successful applications of neural networks in the area of automotive engineering including engine and gearbox control, vehicle handling, modeling nonlinear systems.

An FNN with two hidden layers and one output layer was constructed. For the activation functions of neurons, tangent hyperbolic function was used. The training algorithm gradient decent was utilized for learning of the energy consumption model of the test vehicle. From given data, 75% was used for training,15% was used for validation, and 10% was used for testing. To train the FNN, Machine Learning Toolbox of MATLAB (MATLAB, 2023) was used [28].

Due to confidentially, vehicle parameters are not allowed to be shared.

In summary, the integration of the longitudinal dynamic model, lateral vehicle model, and energy consumption model provides a comprehensive framework for simulating and controlling autonomous vehicle behavior. Each model addresses a specific aspect of vehicle dynamics, from straight-line acceleration to lateral movements and energy efficiency. The interplay between these models enables the development of robust and efficient control algorithms, paving the way for safer and more energy-efficient autonomous vehicles. In the following chapters, we will delve deeper into each model's specifics, exploring their mathematical foundations, implementation details, and practical applications in autonomous driving scenarios.

3.2 Controllers

In this study, the controller system consists of three main parts which illustrated in Figure 3.3: i) GWCS processes the traffic light data, vehicle speed, and position to determine the desired acceleration profile for green wave; ii) vehicle detection uses

the speed and location of the other vehicles in the traffic and the desired speed profile from GWCS to trigger the lane change or set the constrains of the MPC for collision avoidance; iii) the lateral and the longitudinal controllers uses PID and MPC, respectively, to control lateral two-wheel vehicle model and longitudinal dynamics model according to the outputs from vehicle detection and GWCS.

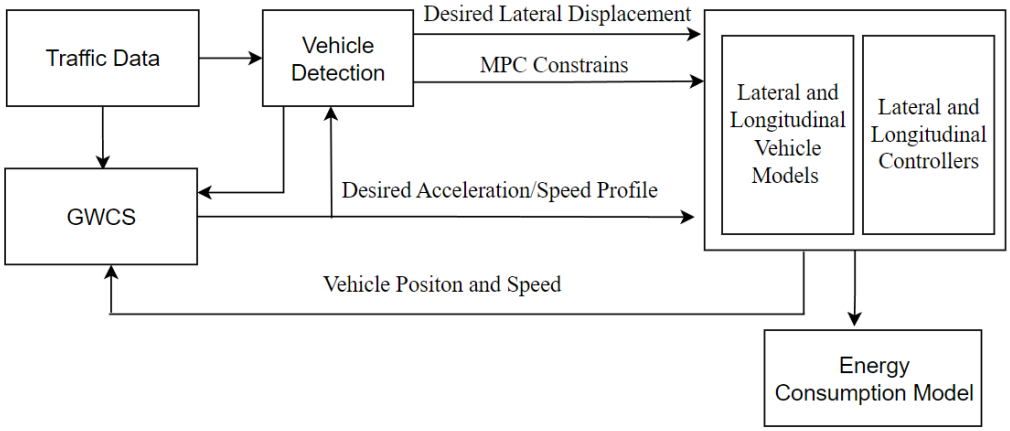

Figure 3.3 Controller System

3.2.1 MPC Controller Design for Longitudinal Vehicle Model

It is expected the vehicle to pass the green lights by controlling the speed based on the determined criteria. Along with the speed control, collision avoidance was also considered.

The vehicle models are first converted to a state-space form and discretized with a sample time t, so that the MPC controller can be designed in discrete time. The vehicle's longitudinal dynamics model in state-space form is:

$$x\,(k+1) = Ax\,(k) + Bu\,(k) + D \tag{3.15}$$

where x (k) is the vehicle's state at the current time step; u(k) is the control applied on the vehicle at the current time step, which includes the vehicle's engine torque and the total brake force

$$u(k) = \begin{bmatrix} T_e(k) \\ F_{brake}(k) \end{bmatrix} = \begin{bmatrix} u_1(k) \\ u_2(k) \end{bmatrix} \tag{3.16}$$

A, B, and D are given as:

$$A = \frac{C_1 - tC_3^*}{C_1} \tag{3.17}$$

$$B = \begin{bmatrix} \frac{C_2 t}{C_1} & -\frac{t}{C_1} \end{bmatrix} = [b_1 \quad b_2] \tag{3.18}$$

$$\mathrm{D} = \frac{tC_4^*}{C_1} \tag{3.19}$$

Following the definitions above, the vehicle's longitudinal dynamic states in a prediction horizon of *p* steps with a given control sequence can be written as:

$$X = \tilde{A}x(k) + \tilde{B}U + \tilde{C}D \tag{3.20}$$

where:

$$X = \begin{bmatrix} x(k+1) \\ x(k+2) \\ \vdots \\ x(k+p) \end{bmatrix} \tag{3.21}$$

$$U = \begin{bmatrix} u_1(k) \\ u_2(k) \\ u_1(k+1) \\ u_2(k+1) \\ \vdots \\ u_1(k+p-1) \\ u_2(k+p-1) \end{bmatrix} \tag{3.22}$$

$$\tilde{A} = \begin{bmatrix} A \\ A^2 \\ \vdots \\ A^P \end{bmatrix} \tag{3.23}$$

$$\tilde{B} = \begin{bmatrix} b_1 & b_2 & 0 & 0 & \cdots & 0 & 0 \\ Ab_1 & Ab_1 & b_1 & b_2 & \cdots & 0 & 0 \\ \vdots & \vdots & \vdots & \vdots & \ddots & \vdots & \vdots \\ A^{p-1}b_1 & A^{p-1}b_2 & A^{p-2}b_1 & A^{p-2}b_2 & \cdots & b_1 & b_2 \end{bmatrix} \tag{3.24}$$

$$\tilde{C} = \begin{bmatrix} 1 \\ A+1 \\ \vdots \\ A^{p-1} + A^{p-2} + \cdots + 1 \end{bmatrix} \tag{3.25}$$

A quadratic cost function was employed to measure the control effort estimation over the prediction horizon. The reduction of desired acceleration and, consequently, the demanded torques from the electric motor immediately impact the consumption of mechanical energy, which eventually affects the amount of electrical energy supplied by the batteries. Acceleration minimization is essentially the act of reducing variances in vehicle speed from its initial value, thereby eliminating expensive acceleration periods. Therefore, the cost function may be expressed in the following manner:

$$J_i(k) = \sum_{t=k}^{N_p-1} u^T R u + (a - a_{ref})^T Q\, a - a_{ref}) \tag{3.26}$$

$$a_{pred} - a_{ref} = \begin{bmatrix} a_1 - a_{ref} \\ a_2 - a_{ref} \\ \vdots \\ a_p - a_{ref} \end{bmatrix} \tag{3.27}$$

R is $2p\ x\ p$ matrix, which forms as:

$$R = \begin{bmatrix} C_4 & 0 & \ldots & 0 \\ 0 & 0 & \ldots & 0 \\ 0 & C_4 & \ldots & 0 \\ \vdots & \vdots & \ddots & \vdots \\ 0 & 0 & \cdots & C_4 \\ 0 & 0 & \cdots & 0 \end{bmatrix} \tag{3.28}$$

As matrix $Q = R\tilde{B} + \widetilde{B^T} B.C_4$ is not symmetric. Q is substituted by $\tilde{Q} = \frac{1}{2}(Q + Q^T)$, which is a commonly adopted technique.

In equation 3.26, the first term represents the control effort, while the second term penalizes any discrepancies between the predicted acceleration and a reference

acceleration. The reference acceleration was selected to ensure that the vehicle reaches the desired location at the desired time. R and Q are matrices utilized to assign relative weights to system inputs and states in order to compute the cost function. In this formulation, weighting matrices were selected with the goal of reducing control signal energy. The cost function was minimized using Quadratic Programming, taking into account different state and control input limitations.

The proposed longitudinal control structure is illustrated in Figure 3.4.

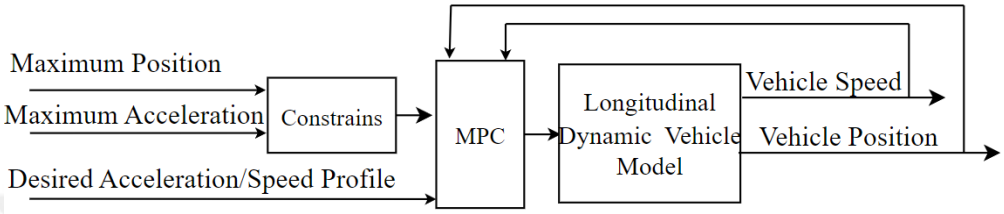

Figure 3.4 Longitudinal Control Structure

A maximum position constraint must be imposed for the safety to ensure that the ego vehicle does not approach the preceding vehicle too closely.

$$\begin{bmatrix} t & 0 & \dots & 0 \\ t & t & \dots & 0 \\ \vdots & \vdots & \ddots & \vdots \\ t & t & \dots & t \end{bmatrix} \begin{bmatrix} x(k+1) \\ x(k+2) \\ \vdots \\ x(k+p) \end{bmatrix} + \begin{bmatrix} 1 \\ 1 \\ \vdots \\ 1 \end{bmatrix} P_{ego}(k) \leq \begin{bmatrix} P_{pre}(k+1) \\ P_{pre}(k+2) \\ \vdots \\ P_{pre}(k+p) \end{bmatrix} - \begin{bmatrix} 1 \\ 1 \\ \vdots \\ 1 \end{bmatrix} d_{min} \quad (3.29)$$

$P_{ego}$is the ego vehicle's positon at current time step; P_{pre} is predicted vehicle position d_{min} is the allowed distance between the ego and preceding car.

In order to reduce the rapid accelerations and de-accelerations, the acceleration is limited as;

$$-2m/s^2 \leq a \leq 3m/s^2$$

In order the select the prediction horizon, different length of prediction horizons is tested. Including 5s, 10s, 15s, 20s, and 25s. The results are shown in the Figures 3.5, 3.6 and 3.7.

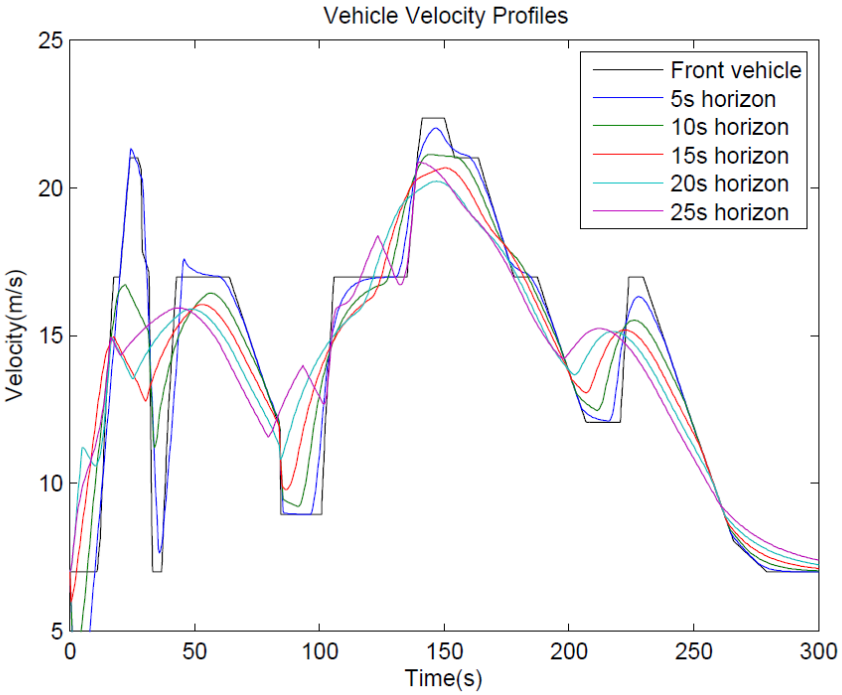

Figure 3.5 Speed Profiles with Different Horizons

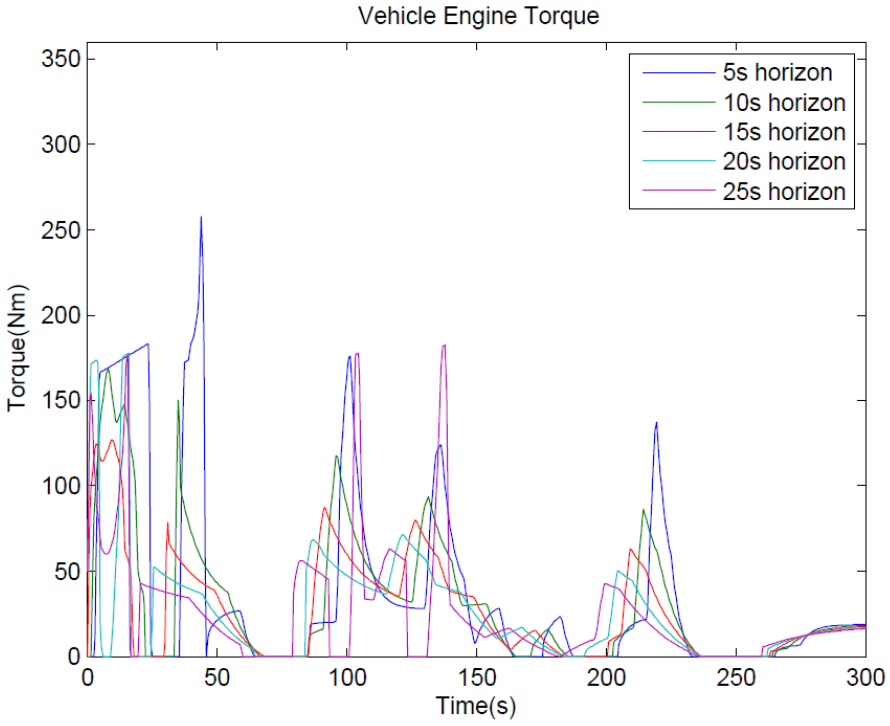

Figure 3.6 Requested Torque with Diffrent Horizons

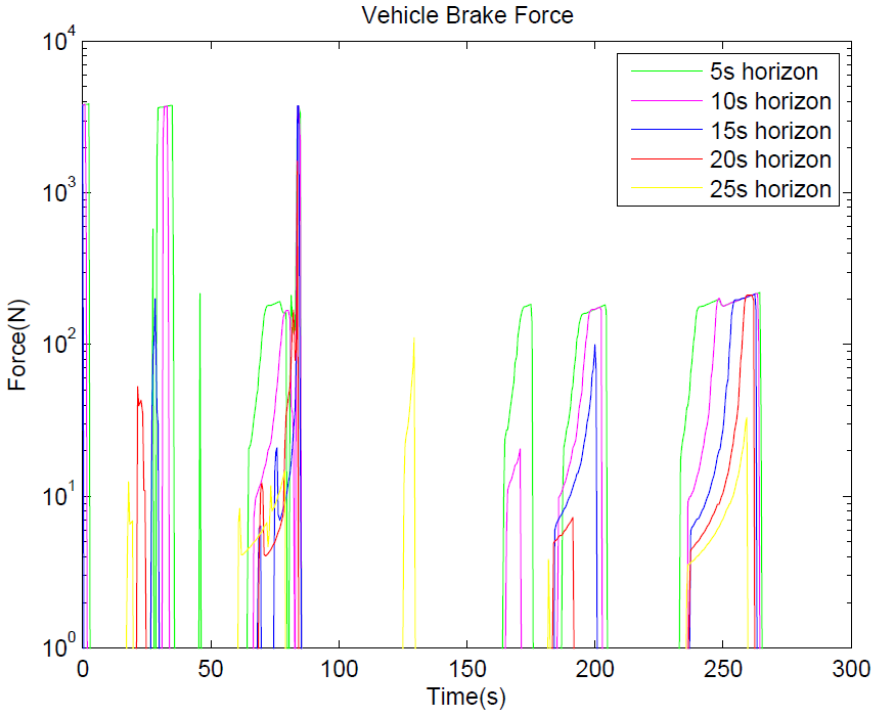

Figure 3.7 Applied Break Force with Different Horizons

Figure 3.5 illustrates that the MPC-controlled ego vehicle exhibits much reduced sensitivity to variations in the preceding vehicle's speed with extended prediction horizons. Extended prediction horizons enable the algorithm to anticipate the vehicle's speed adjustments in advance of actual changes. The magnitude of the vehicle's engine torque and braking force diminishes as the prediction horizon extends, as seen in Figure 3.6 and Figure 3.7. Considering the computation effort and the acceleration profile the prediction horizoncan be selected between 10s and 20s.

3.2.2 PID Controller Design for Lateral Vehicle Model

In this study, the objective is to achieve precise path following for a vehicle, facilitated by the implementation of a PID controller within the lateral vehicle dynamics model. The PID controller is a feedback control mechanism crucial for minimizing yaw rate errors and enhancing trajectory tracking performance.

The context of lateral vehicle dynamics, the PID controller modulates the yaw moment, which directly correlates with wheel torque adjustments necessary to minimize yaw rate errors. The relationship between yaw moment and wheel torque can be represented as:

$$M = \frac{l}{2}\left(\frac{-T_{mrl} \pm T_{mrr}}{r_w}\right) \tag{3.30}$$

$$T_{mrl} = T_{st} - \frac{r_w}{d} M \tag{3.31}$$

$$T_{mrr} = T_{st} + \frac{r_w}{d} M \tag{3.32}$$

where T_{st} indicates the driving torque and wheel radius is r_w.

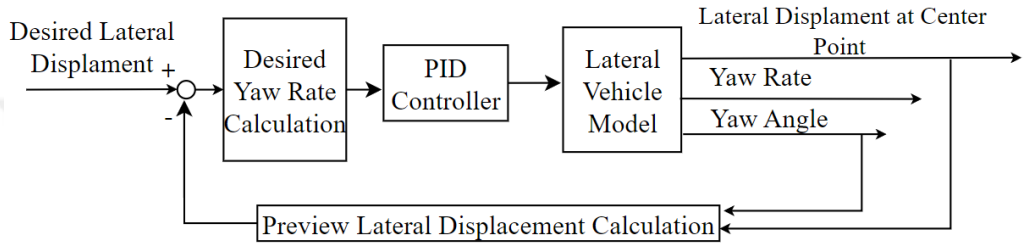

Figure 3.8 Lateral Controller Structure

Desired lateral displacement is calculated when vehicle changes the lane. The path to be followed by the vehicle represents a single lane change behavior and is described by a Bézier curve. An n-th curve of degree Bézier is defined by a total of n+1 control points, ranging from P_0 to P_1 [29-31], as shown in equation 3.33:

$$P(t) = \sum_{i=0}^{n} B_{i,n}(t) p_i, t \in [0,1] \tag{3.33}$$

where, t is normalized time parameter, B_i is i_{th} control point location of Bézier curve, and $P(t)$ indicates the coordinate vector in i_{th} control point.

In the simulations, the Bézier curve with four control points shown in Figure 3.9 was used [26].

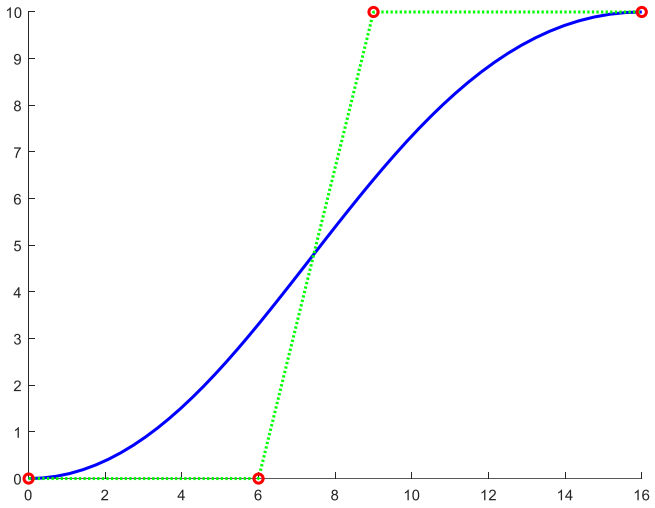

Figure 3.9 Bézier Curve with Four Control Point

Desired lateral displacement in the form of Bézier Curve is calculated every time vehicle needs to change the lane based on its current vehicle speed. The speed and torque losses while changing the lane are neglected.

The PID gains are critical parameters that must be carefully tuned to optimize performance across varying driving conditions. In this study, the tuning process is facilitated using the Genetic Algorithm Toolbox in MATLAB. This toolbox allows for automated or semi-automated optimization of PID controller parameters based on predefined performance criteria and constraints.

Table 3.1 Optimization Toolbox Parameters

Parameter	Value
Lower and Upper bound	**[-10000, 10000]**
Population type and size	**Double Vector, 50**
Creation function	**Uniform**
Initial range	**-10 to 10**

Table 3.2 Optimization Toolbox Parameters (continued…)

Scaling and Selection function	**Rank, Tournament**
Tournament size	**4**
Mutation and Crossover function	**Adaptive feasible, Heuristic**
Crossover function	**Heuristic**
Migration direction	**Forward**
Migration fraction and interval	**0.2, 20**
Nonlinear constraint algorithm	**Augmented Lagrangian**
Initial penalty, Penalty factor	**10, 100**
Maximum number of generations	**100**

For different vehicle speeds, 10 m/s, 20 m/s, and 30 m/s, Lateral and longitudinal displacements and torque demand can be seen in Figures 3.10, 3.11, and 3.12.

In higher speed values the overshoot error decreases. There errors are 12.7% at 10 m/s 8.45% at 20 m/s and 5.12% at 30 m/s .This could be improved by tuning the PID controller.

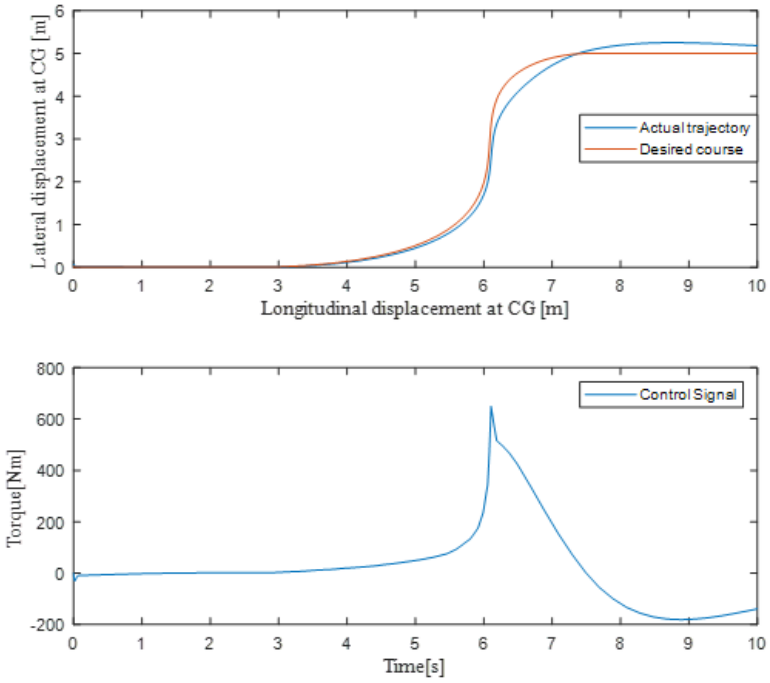

Figure 3.10 Lateral and Longitudinal Displacement , Torque Demand at Vehicle Speed 10 $\boldsymbol{m/s}$

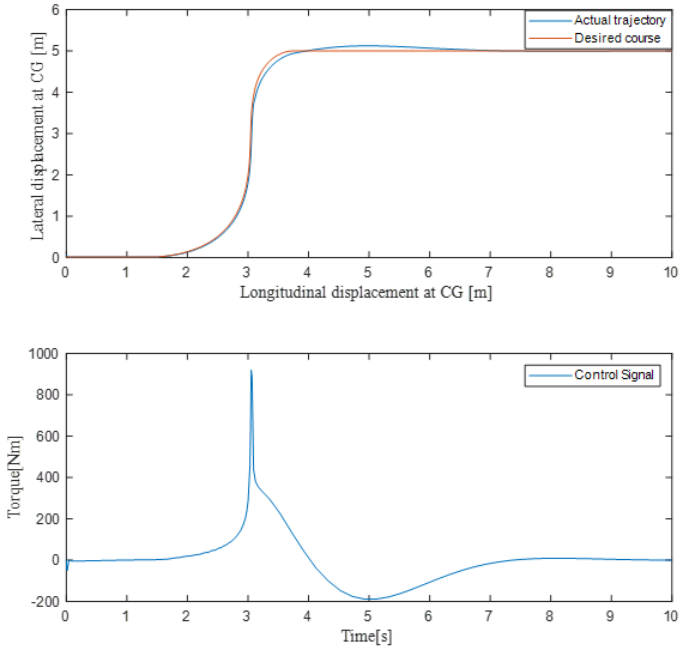

Figure 3.11 Lateral and Longitudinal Displacement , Torque Demand at Vehicle Speed 20 $\boldsymbol{m/s}$

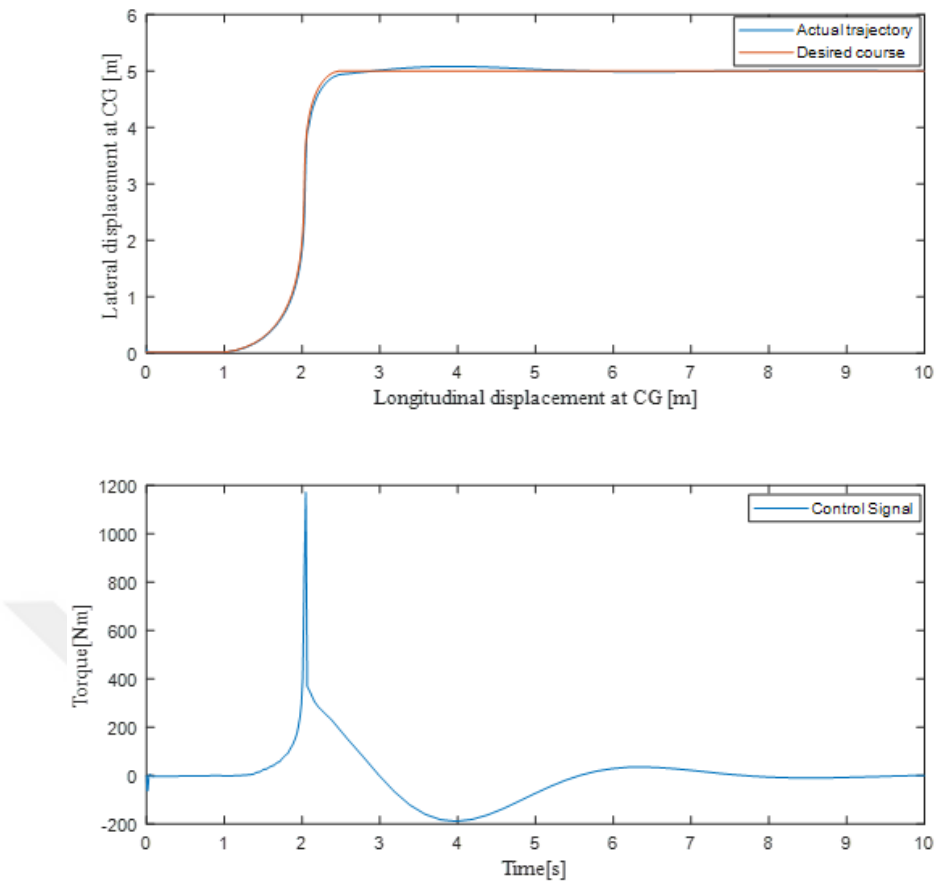

Figure 3.12 Lateral and Longitudinal Displacement , Torque Demand at Vehicle Speed 30 $\boldsymbol{m/s}$

In conclusion, integrating a PID controller calibrated with the Genetic Algorithm Toolbox in MATLAB significantly enhances the vehicle's ability to follow a desired path accurately. By minimizing yaw rate errors through well-tuned proportional, integral, and derivative actions, the PID controller plays a crucial role in advancing both driver assistance systems and autonomous driving technologies. This approach not only improves vehicle maneuvering capabilities but also contributes to safer and more efficient navigation through complex driving environments.

4
GREEN WAVE OPTIMIZATION ALGORITHM

This chapter addresses the problem of finding an optimal speed or acceleration profile for vehicles passing through a series of traffic lights, considering multiple green phases and varying speed or acceleration limits. The primary objective is to minimize the total speed or acceleration variation between consecutive traffic lights while ensuring that the chosen speeds or accelerations lie within the allowed limits for each green phase.

In order to select the between speed profile and acceleration profile small simulation is constructed. In this simulation two vehicles, vehicle V_1 and V_2, starts at the same position. Vehicle V_1 will use speed setpoint from the start to reach the end of the road and vehicle V_2 will use acceleration setpoint to reach the end of the road.

For 1000 m road vehicle V_1 and V_2 have 0 m/s at $t = 0s$. Both of the vehicle V_1 and V_2 needs to be at end of the road at $t = 100s,\ 50s,$ and $20s$. V_1 will accelerate with maximum acceleration 3 m/s^2 for time t_a which will be calculated as follows

$$\mathrm{x} = V_0 t_a + \frac{1}{2} a {t_a}^2 + (V_0 + a t_a)(t - t_a) \tag{4.1}$$

$$1000\ \mathrm{m} = \frac{3}{2} {t_a}^2 + (3t_a)(t - t_a) \tag{4.2}$$

$$2000\ \mathrm{m} = 6t_a t - 3{t_a}^2 \tag{4.3}$$

Then the speed setpoint V_{1sp} for V_1

$$V_{1sp} = 3t_a \tag{4.4}$$

For V_2 accelartion speed point a_{sp} calculated as

$$\mathrm{x} = V_0 t + \frac{1}{2} a_{sp}\, t^2 \tag{4.5}$$

$$1000 \text{ m} = a_{sp}\, t^2 \tag{4.6}$$

$$a_{sp} = \frac{2000}{t^2} \tag{4.7}$$

Based on these calculations above, we can calculate the energy consumption with the help of FNN.

Table 4.3 Optimization Toolbox Parameters

Vehicle and Time to reach	Energy Consumption (Watt)
$\boldsymbol{V_1 - 100s}$	121.4
$\boldsymbol{V_2 - 100s}$	109.4
$\boldsymbol{V_1 - 50s}$	210.57
$\boldsymbol{V_2 - 50s}$	189.78
$\boldsymbol{V_1 - 25s}$	345.4
$\boldsymbol{V_2 - 25s}$	301.6

The energy consumption for different reach times can be seen in Table 4.1. The energy consumption varies depending on the reach time. By using the acceleration for whole road energy consumption can be reduced between 5.4% to 9.8%. Since the main goal of our optimization is to reduce the energy consumed, the acceleration setpoint is selected for the optimization.

4.1 Problem Formulation

The problem can be formally described as follows: Given a sequence of traffic lights, each having multiple green phases with specified minimum and maximum acceleration limits, we aim to determine the optimal acceleration profile for a vehicle. The selected acceleration for each traffic light should:

1. Lie within the range of speed limits for any of the green phases at that light.
2. Minimize energy consumption between consecutive traffic lights.

4.2 Light Phase Calculation

In order to find a minimum and maximum acceleration profile for each light following calculation needs to be made:

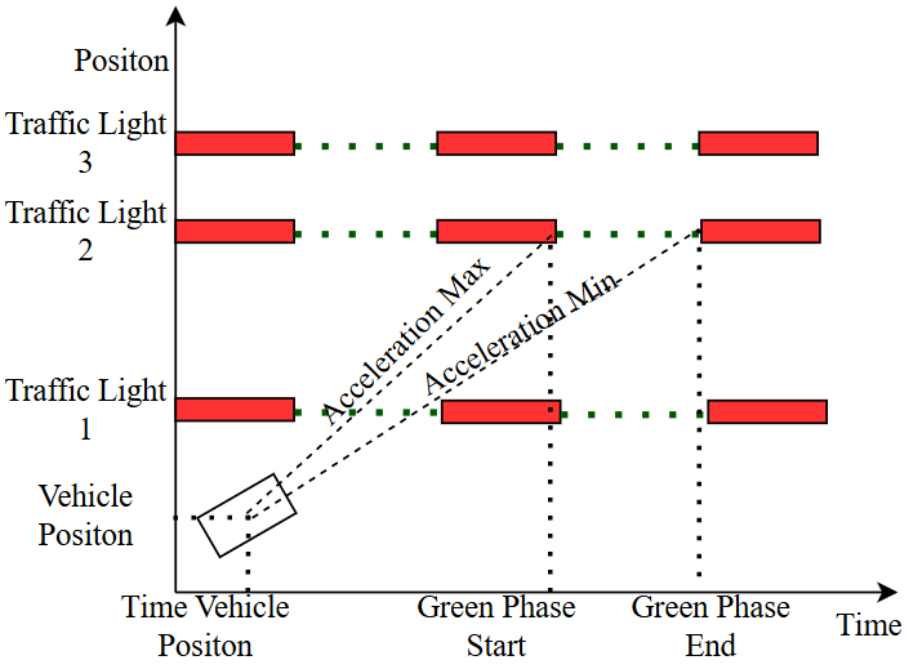

Figure 4.1 Minimum and Maximum Acceleration Profiles

Defining X_{Veh} is the position of the vehicle, T_{Veh} is time that the vehicle is at that position and V_{Veh} is speed of the vehicle; assuming vehicle knows position of each traffic light X_{TLn}, the green phase start time $T_{TLn_{k1}}$ and the green phase stop time $T_{TLn_{k2}}$ thanks to the V2X communication, where n is number of lights and k is number of green phases, we arrive at

$$G_{TL} = \begin{bmatrix} [T_{TL1_1 1}, T_{TL1_1 2}] & \dots & [T_{TL1_k 1}, T_{TL1_k 2}] \\ \vdots & \ddots & \vdots \\ [T_{TLn_1 1}, T_{TLn_1 2}] & \dots & [T_{TLn_k 1}, T_{TLn_k 2}] \end{bmatrix} \tag{4.8}$$

$$\Delta X_{TL} = [X_{TL1} - X_{Veh} \quad \dots \quad X_{TLn} - X_{Veh}] \tag{4.9}$$

where G_{TL} is a matrix which contains the information of each light green phase start and stop time. ΔX_{TL} is the position difference between the car and each traffic light.

By using the equation 4.5, the minimum and maximum accelerations are calculated and held by

$$G_a = \begin{bmatrix} [a_{TL1_1 1}, a_{TL1_1 2}] & \cdots & [a_{TL1_k 1}, a_{TL1_k 2}] \\ \vdots & \ddots & \vdots \\ [a_{TLn_1 1}, a_{TLn_1 2}] & \cdots & [a_{TLn_k 1}, a_{TLn_k 2}] \end{bmatrix} \quad (4.10)$$

where G_a is a matrix containing the speed information that required to pass the car through the green phase. $a_{TLn_{k1}}$ and $a_{TLn_{k2}}$ are the maximum and minimum accelerations required to pass through the green phases of the lights.

The G_a means each traffic light i is characterized by a set of green phases, with each phase p having a minimum and maximum allowed speed:

$$\text{Speed limit for phase } p \text{ of light } i\text{: } [a_{i,p}^{min}, a_{i,p}^{max}]$$

Where $a_{i,p}^{min}$ is the minimum speed for phase p and $a_{i,p}^{max}$,s the maximum speed. The objective is to select a speed a_i for each traffic light i such that $ai \in [a_{i,p}^{min}, a_{i,p}^{max}]$ for some phase p, and the total speed change between consecutive traffic lights is minimized.

The G_a is filtered by following rules to ease the computation effort for dynamic programming:

For each minimum and maximum acceleration values $[a_{i,p}^{min}, a_{i,p}^{max}]$ in G_a

- If both $[a_{i,p}^{min}, a_{i,p}^{max}]$ are higher than $a_{max} = 3\ m/s^2$ or lower than $a_{min} = -2\ m/s^2$, the light phase it removed from matrix.
- If any one of $[a_{i,p}^{min}, a_{i,p}^{max}]$ within the $[a_{max,}a_{mix}]$limits but the other one is not in the limits, the one which is not in the limit will be limited by the closest limit(either $a_{max,}\ or\ a_{mix}$).
  Example: $[2\ m/s^2, 3.7\ m/s^2]$ -> $[2\ m/s^2, 3\ m/s^2]$
- If both $[a_{i,p}^{min}, a_{i,p}^{max}]$ would increase the vehicle speed higher than $V_{max} = 25\ m/s$(90 km/h) or lower than $V_{min} = 0\ m/s$, timing for that the light phase it removed from matrix. This is calculated as : $V_{pred} = V_{Veh} +$

$\frac{1}{2}a\,.\,(T_{TL} - T_{Veh})$as V_{pred} is the speed that the car will reach when it's at the light T_{TL} light phase start or stop time depending of $a_{i,p}^{min}$ *or* $a_{i,p}^{max}$.

- If any one of $[a_{i,p}^{min}, a_{i,p}^{max}]$ would increase the vehicle speed more than $V_{max} = 25\ m/s$(90 km/h) or $V_{min} = 0\ m/s$ the exceeding limit will be re-calculated as $X_{TL1} - X_{Veh} = V_{Veh}\,(T_{TL} - T_{Veh}) + \frac{1}{2}a_{new}\,(T_{TL} - T_{Veh})^2$

As an example scenario:

- Vehicle's current position $X_{Veh} = 100\ m$
- Vehicle's current time $T_{Veh} = 10\ s$
- Vehicle's Current Speed $V_{Veh} = 15\ m/s$

Three traffic lights with two green phases

- Light Locations $X_{TL} =$ [300 600 900] m
- Light phases for three lights
  - $G_{TL} = \begin{bmatrix} [15,25] & [40,50] \\ [20,30] & [70,80] \\ [20,30] & [70,80] \end{bmatrix}$ s
- $\Delta X_{TL} =$ [200 500 800] m
- $G_a(1,1,1) = \frac{2\,(\Delta X_{TL}(1) - (V_{Veh} - (G_{TL}(1,1,1) - T_{Veh})}{(G_{TL}(1,1,1) - T_{Veh})^2} = \frac{2\,(200 - (15 - (15 - 10)}{(15 - 10)^2} = 2\ m/s^2$
- Step above is calculated for each element in G_{TL} as assigned to G_a
  - $G_a = \begin{bmatrix} [2, -0.22] & [-0.56, -0.5] \\ [1, -0.22] & [-0.28, -0.28] \\ [11,2] & [-0.056, -0.1] \end{bmatrix} m/s^2$
- Then G_a is filtered according to the rules;
  - Only $G_a(3,1,1)$ the acceleration for 3rd Light 1st phase maximum acceleration (11 m/s^2) is out of bounderies. It is reduced to 3 m/s^2.
  - New $G_a(1,1,1)$ *and* $G_a(1,1,2)$ setpoint will make the vehicle lower than 0 m/s . They are removed from matrix.
    - $V_{pred} = V_{Veh} + G_a(1,1,1).\,(G_{TL}(1,1,1) - T_{Veh}) = 15 - 0.56.\,(40 - 10) = -0.9\ m/s$
    - $V_{pred} = V_{Veh} + G_a(1,1,2).\,(G_{TL}(1,1,2) - T_{Veh}) = 15 - 0.5.\,(50 - 10) = -5\ m/s$
  - New $G_a(2,2,1)$ *and* $G_a(2,2,2)$ setpoint will make the vehicle lower than 0 m/s . They are removed from matrix.

        - $V_{pred} = V_{Veh} + G_a(2,2,1).(G_{TL}(2,2,1) - T_{Veh}) = 15 - 0.27.(70 - 10) = -1.8\ m/s$
        - $V_{pred} = V_{Veh} + G_a(2,2,2).(G_{TL}(2,2,2) - T_{Veh}) = 15 - 0.28.(80 - 10) = -3.9\ m/s$
        -
    - New $G_a(3,1,1)\ and\ G_a(3,1,2)$ setpoint will make the vehicle go faster than $25\ m/s$. They are removed from matrix.
        - $V_{pred} = V_{Veh} + G_a(3,1,1).(G_{TL}(3,1,1) - T_{Veh}) = 15 + 3.(20 - 10) = 45\ m/s$
        - $V_{pred} = V_{Veh} + G_a(3,1,2).(G_{TL}(3,1,2) - T_{Veh}) = 15 + 2.(30 - 10) = 55 m/s$

- Filtered $G_a = \begin{bmatrix} [2, -0.22] & [inf, inf] \\ [1, -0.22] & [inf, inf] \\ [inf, inf] & [-0.1, -0.056] \end{bmatrix}$.

4.3 Objective

The objective function to be minimized can be written as:

$$Minimize \sum_{i=2}^{n} f_{e\_cost}(a_i, a_{i-1}, x_i, x_{tf}, v_0, t_i, t_0) \quad (4.11)$$

where a_i represents the selected acceleration at traffic light i, n is the total number of traffic lights, x_i position of the vehicle when the algorithm has triggered, x_{tf} is the postion of the next traffic light, v_0 speed of position of the vehicle when the algorithm has triggered, t_i selected time of green phase, $t_0$time of position of the vehicle when the algorithm has triggered.f_{e_cost} is a function that calculates the energy consumption of the vehicle with the help of NN model

4.4 Approach

The approach to solving this problem involves using dynamic programming to explore different acceleration options for each traffic light. Each traffic light has multiple green phases, and for each phase, we need to explore the range of allowed

acceleration. To avoid an exhaustive search across all possible acceleration, we discretize the acceleration ranges and apply a dynamic programming algorithm that minimizes energy consumption.

4.4.1 Discretization of Acceleration Limits

Instead of evaluating every possible real number between the minimum and maximum speed limits, we discretize the speed ranges into a finite set of values. The step size Δa controls the granularity of this discretization:

$$Acceleration\ options\ for\ phase\ p\ of\ light\ i: \{a_{i,p}^{min}, a_{i,p}^{min} + \Delta a, \dots, a_{i,p}^{max}\}$$

the step size Δa can be chosen based on a trade-off between accuracy and computational efficiency. A smaller Δa provides higher accuracy but increases the computational cost. Δa is selected as 0.01 for optimal accuracy and computational cost.

4.5 Dynamic Programming Formulation

To solve the problem, we define a dynamic programming table $dp[i][p][j]$, where:

- i is the index of the traffic light.
- p is the phase at the current light.
- j is the acceleration index within the discretized speed options for phase p.

The value $dp[i][p][j]$ stores the minimum cumulative acceleration change from the first traffic light to the current light i, for phase p and speed j. The recurrence relation for the dynamic programming formulation is:

$$dp[i][p][j] = min_{q,k}(dp[i-1][q][k] + f_{\text{e\_cost}}(a_i, a_{i-1}, x_i, x_{tf}, v_0, t_i, t_0)) \qquad (4.12)$$

where q and k represent the phase and speed index for the previous light $i-1$.

4.6 Implementation

The dynamic programming approach was implemented in MATLAB. The input consists of a cell array where each element represents a traffic light and contains the minimum and maximum acceleration limits for each green phase. The acceleration limits are discretized based on a specified step size, and the dynamic

programming algorithm evaluates all possible speed transitions between consecutive lights to minimize total energy consumption. The Pseudo code can be seen as below:

- Set n as the number of traffic lights.
- Create an array acc_options to store the discretized acceleration for each phase at every light.
- For each traffic light `i` from `1` to `n`:
    - For each phase `p` of traffic light `i`:
        - Set `min_acc = acc_limits[i][p][1]`
        - Set `max_acc = acc_limits[i][p][2]`
        - Discretize the speed range from `min_acc` to `max_acc` using `step_size`.
        - Store the discretized acceleration in `acc_options[i][p]`.
- Create a DP table dp[i][p][j], where:
    - i is the index of the traffic light.
    - p is the phase at the current light.
    - j is the acceleration index within the discretized acceleration for that phase.
- Set dp[i][p][j] = ∞ for all lights, phases, and accelerations to represent an initially high cost.
- For the first traffic light i = 1:
- For each phase p of the first light:
    - For each acceleration j in acc_options[1][p]:
        - Set dp[1][p][j] = 0 (no acceleration changes for the first light).
- For each traffic light i from 2 to n:
    - For each phase p_curr of light i:
        - For each acceleration s_curr in acc_options[i][p_curr]:
            - For each phase p_prev of the previous light (i-1):
                - For each speed s_prev in acc_options[i-1][p_prev]:
                    - Calculate the speed change:
                        - cost = dp[i-1][p_prev][s_prev] + $f_{\text{e\_cost}}(a_i, a_{i-1}, x_i, x_{tf}, v_0, t_i, t_0)$

            - If cost < dp[i][p_curr][s_curr], update:
                - dp[i][p_curr][s_curr] = cost
                - Store the index of the previous accelerations s_prev for backtracking:
                    - selected[i][p_curr][s_curr] = (p_prev, s_prev).
    - Initialize minAccChange = ∞
    - For the last traffic light i = n:
        - For each phase p and acc j:
            - If dp[n][p][j] < minSpeedChange:
                - Set minAccChange = dp[n][p][j]
                - Store the optimal last_phase = p and last_speed = j.
    - Set acc_profile[n] = acc_options[n][last_phase][last_speed].
    - For each traffic light i from n-1 down to 1:
        - Use selected[i+1][last_phase][last_speed] to find the previous optimal accelerations:
            - speed_profile[i] = selected[i+1][last_phase][last_speed].
        - Update last_speed accordingly.
    - Return minAccChange and the acc_profile containing the optimal accelerations for all traffic lights.

Continuing the example calculations from Chapter 4.2:

- $G_a = \begin{bmatrix} [2, -0.22] & [-0.5, -0.56] \\ [1, -0.22] & [inf, inf] \\ [inf, inf] & [-0.1, -0.05] \end{bmatrix} m/s^2$
- Number of lights n= 3 light phases p=1
- acc_options[1,1] = $[[2, 1.99,\ 1.98, \dots, 0, \dots -0.21, -0.22]]$
  acc_options[2,1] = $[1, 0.99,\ 0.98, \dots, 0, \dots -0.21, -0.22]$
  acc_options[3,1] = $[[-0.1, -0.09, -0.08, \dots -0.04, -0.05]]$

- For the 1st light there is no previous light so calculated the minimum energy cost for all options selected acceleration is -0.22 with lowest energy of 5.45 W.
- For each element in acc_options[2,1] we calculate the cost considering selected acceleration for 1st light is -0.22. First selected cost is added to selection options cost to reduce the computation.
    - dp[2][1] = [21.4 , 20.45 , 20.1 …… 11.98]
- For each element in acc_options [2,1] the calculate cost for each element in acc_options [3,1] which becomes a matrix [1x616] maxtix.
    - dp[3][1] = [30.4, 30.45 , 31.1 …… 40.48]
- In dp[3][1] the lowest value is 30.4 which is the 1st element of the array. If we do back tracking with this value we can find the set points as:
    - minAccChange = [-0.22 -0.22 -0.1]
- Since last element of the setpoint matrix is different from other we cannot make sure the last setpoint will be valid. For last setpoint we re-calculate the speed and position and the G_a matrix.
    - $X_{new} = 600\ m$ since vehicle would pass the 2nd light
    - Vehicle's current time $T_{new} = 30\ s$ since vehicle would pass the 2nd light with minimum acceleration.
    - $V_{new} = 15 - 0.22 * (30 - 10) = 10.6\ m/s$
    - New G_{TL} = [70 80] since first phase was [20,30] and where at T= 30
    - New G_a = $[[-0.15, -0.18]]\ m/s^2$
- With new G_a calculated new set point would be -0.18 m/s^2
    - Then minAccChange = [-0.22 -0.22 -0.18] which would be our new acceleration set points.

In this chapter, we addressed the problem of optimizing vehicle accelerations profiles through a sequence of traffic lights with multiple green phases. By using dynamic programming and discretizing the accelerations limits, we were able to minimize the energy consumption between consecutive traffic lights.

5
SIMULATIONS

5.1 FTP-75 Cycle

The FTP-75, initially designed for evaluating traditional internal combustion engine cars, is also suitable for analyzing electric vehicles (EVs). The FTP-75 test cycle is meant to replicate urban driving situations that mostly involve internal combustion engines. However, its structure and specifications also allow for the evaluation of electric vehicle performance. The test for electric cars evaluates characteristics such as energy consumption and emissions (where relevant) in controlled environments, offering vital insights into the efficiency of EVs and their compliance with regulations.

The characteristics of the cycle are:

- Distance travelled: 11.04 miles (17.77 km)
- Duration: 1369 seconds
- Average speed: 31.5 km/h
- Maximum speed: 91.2 km/h

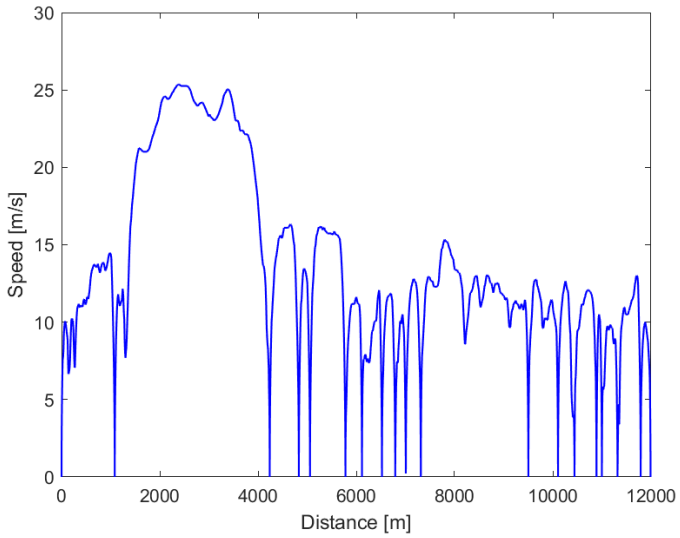

Figure 5.1 Federal Testing Procedure 75 Speed and Distance Profile

5.2 Traffic Light Generation

FTP-75 cycle serves as both a standardized test for evaluating vehicle performance and a reliable foundation for producing realistic traffic scenarios. The FTP-75 is specifically designed to replicate the conditions of driving in urban areas. It accurately records the time when vehicles come to a halt and start again, thereby capturing the frequent stopping and starting that is characteristic of city traffic. The timestamps are crucial for accurately mimicking the behavior of traffic lights in metropolitan areas where crossings are regulated by traffic signals.

By utilizing FTP-75 data, the time at which the vehicle stops are considered as the initiation of a red light period at junctions, whilst the start times reflect the commencement of green light periods. This data enables the reconstruction of whole traffic light cycles. To effectively model genuine traffic flow dynamics, randomized intervals (usually ranging from 60 to 120 seconds) can be used for the red, yellow, and green phases of traffic lights. These intervals mimic the variability observed in real-world traffic light switching periods.

Simulated junctions are set up according to the stop and start events of the FTP-75 cycle, which simulate certain scenarios in the urban environment. This method incorporates the use of several intersection designs and placements of traffic lights to replicate a wide range of traffic situations commonly found in urban areas. The capacity to produce traffic signal sequences in real-time using FTP-75 data facilitates several applications, including autonomous vehicle testing, urban planning, and traffic flow management.

In order to generate the traffic lights, the FTP cycle data of AVL's test vehicle is used. The speed of the vehicle can be seen in Figure 5.2.

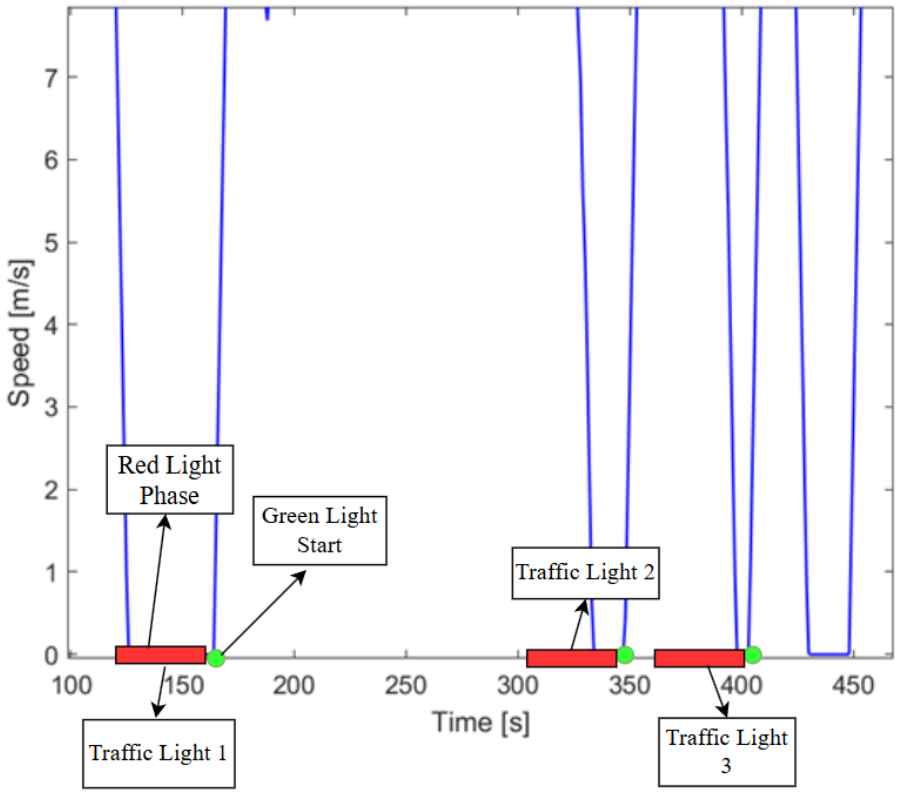

Figure 5.2 Traffic Light Generation from FTP-75 Cycle Data

Essentially, this technology allows for precise and accurate simulations to assess how autonomous cars respond to traffic signals and tactics for managing intersections. Additionally, it aids urban planners in assessing road infrastructure designs and enhancing traffic management strategies by accurately simulating various layouts and traffic densities. Furthermore, this technique simplifies the process of creating and confirming algorithms that are designed to improve the efficiency of traffic flow and decrease congestion in metropolitan regions

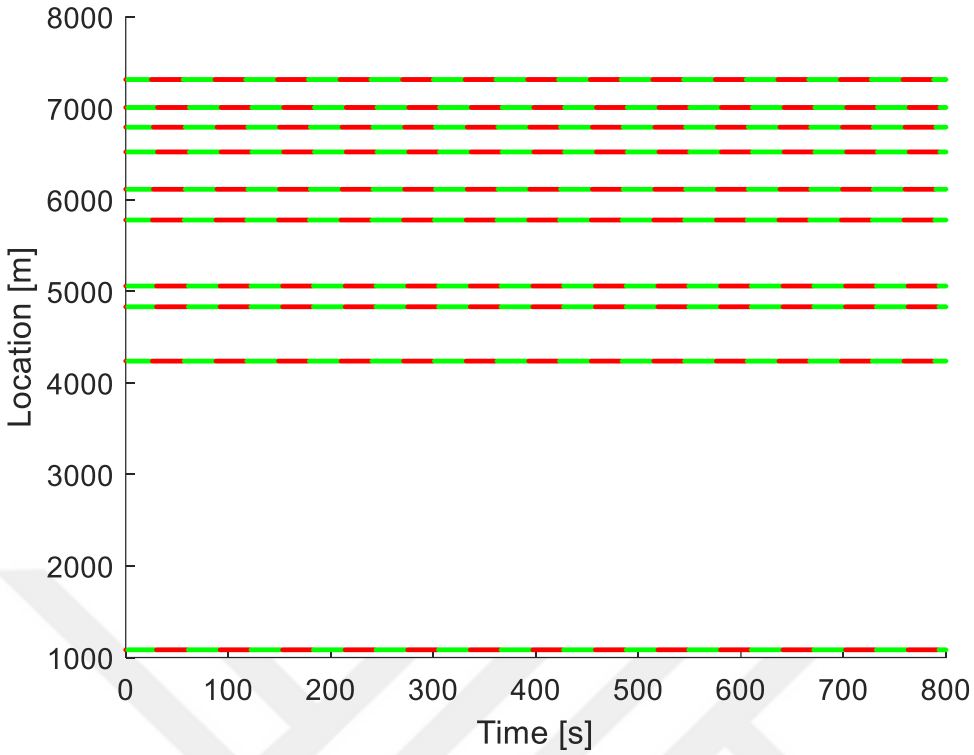

Figure 5.3 Generated Traffic Light Location and Phases

In Figure 5.2, a traffic light is generated when vehicle is standing still in FTP-75 cycle. For phasing red-green lights, time of the green light start $T_{TLx}$is taken as a reference and lights phases change between [60, 120] seconds. In Figure 5.3, the generated TL cycles and locations can be seen.

5.3 Intelligent Driver Model

The Intelligent Driver Model (IDM) is an advanced behavioral model employed for simulating the interactions between automobiles in traffic, especially in crowded settings. The car-following behavior is simulated by taking into account the acceleration dynamics, safety distance from the preceding vehicle, desired speed, and comfortable deceleration rates of each vehicle. By integrating these aspects, the IDM effectively reproduces real-world traffic scenarios and aids researchers in comprehending traffic flow dynamics and congestion patterns.

Essentially, the IDM is utilized in traffic simulation software for the purposes of urban planning, transportation engineering, and the advancement of autonomous vehicle technology. It offers valuable information on enhancing traffic management tactics, such as adaptive cruise control systems and traffic signal timings, to

enhance overall traffic efficiency and safety. The IDM is essential in the development of intelligent transportation systems that can effectively manage different traffic volumes and improve the safety and dependability of future mobility solutions. It achieves this by mimicking how drivers adapt their speed and spacing in response to changing conditions.

IDM explains the dynamics of a single vehicle's position and speed [33]:

$$\dot{v}_\alpha = a^\alpha \left[1 - \left(\frac{v_\alpha}{{v_0}^\alpha}\right)^\delta - \left(\frac{s^*(v_\alpha, \Delta v_\alpha)}{s_\alpha}\right)^2\right] \tag{5.1}$$

$$s^*(v_\alpha, \Delta v_\alpha) = {s_0}^\alpha + {s_1}^\alpha \sqrt{\frac{v}{{v_0}^\alpha}} + T^\alpha v + \frac{v\Delta \mathrm{v}}{2\sqrt{a^\alpha b^\alpha}} \tag{5.2}$$

$$s_\alpha = x_{\alpha-1} - x_\alpha - l_\alpha \tag{5.3}$$

$$\Delta v_\alpha = v_\alpha - v_{\alpha-1} \tag{5.4}$$

In equation 5.1 and 5.2, for vehicle α , $v_\alpha$represents the speed and x_α represents to position at the time t. l_α is length of the vehicle. s_α is the net distance between α and $\alpha - 1$. Δv_α is the velocity difference

To evaluate the performance and effectiveness of our algorithm, it is essential to benchmark it against a well-established model. In this study, we have chosen to use the IDM as a benchmark for our simulations. IDM is widely recognized in traffic flow and vehicle dynamics research for its realistic modeling of driver behavior under various traffic conditions

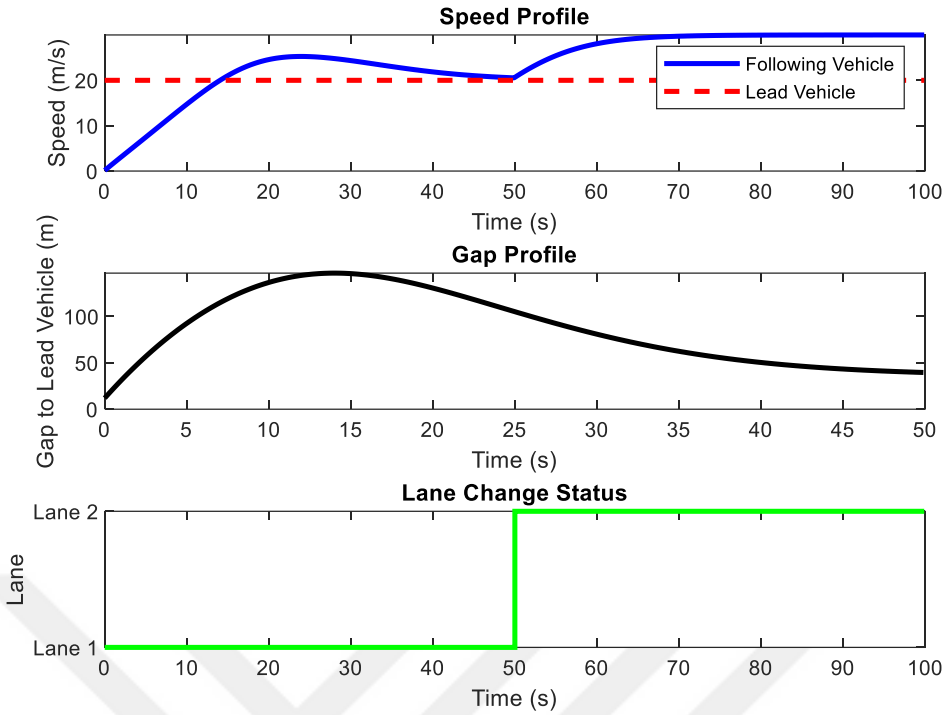

Figure 5.4 IDM Model Results

The following vehicle which controlled by IDM adjusts its speed and maintains a safe distance from the lead vehicle based on parameters like maximum acceleration, desired speed, and the minimum gap required. When the gap between the following vehicle and the lead vehicle falls below a certain threshold, the following vehicle initiates a lane change, after which it accelerates freely towards its desired speed, no longer influenced by the lead vehicle. The simulation tracks and visualizes the speed, gap, and lane change status over time, providing insights into the dynamics of car-following and lane-changing behaviors in traffic. In following simulation IDM model considers red light phase as an object.

5.4 Lane Change Rules

The lane-changing behavior in this model is governed by a set of rules designed to ensure safe and efficient transitions between lanes. A lane change is triggered when the gap between the following vehicle and the lead vehicle becomes smaller than a predefined threshold. This threshold is calculated based on ‘3 Second Rules’ which is based on Conference of European Director of Roads (CEDR) and calculated as follows:

$$P_{lead} - P_{ego} \leq 3\,(V_{ego} - V_{lead}) + \frac{9}{2}\,a_{ego} \tag{5.5}$$

where P_{lead} is the positon of lead car, P_{ego} position of following car, V_{ego} is the speed of following car and a_{ego} is the acceleration of following car.

Upon detecting defined condition in 5.5, the vehicle evaluates whether it is safe to switch to an adjacent lane. Before initiating the lane change, the vehicle ensures that there is enough space in the target lane and that no vehicles are present within a critical distance. If the conditions are met, the vehicle initiates the lane change [34-37].

It is assumed that the ego vehicle gets the speed and position information of six cars in its radius by using V2X communication. This is illustrated in Figure 5.5.

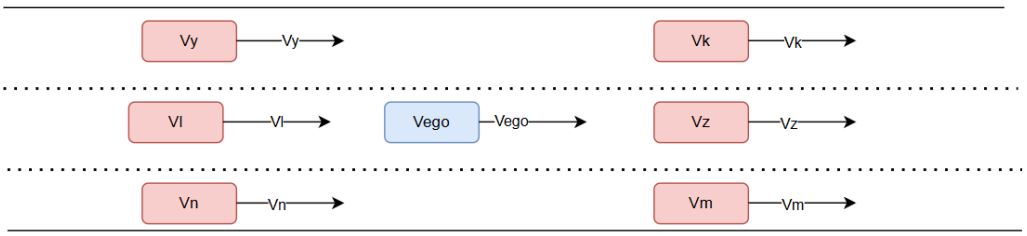

Figure 5.5 Vehicle Information by V2X

where;

P_{ego} position of ego car,

V_{ego} speed of ego car,

P_y position of Car Y which is the left lane behind the ego car,

V_y speed of Car Y,

P_k position of Car K which is left lane in front of the ego car,

V_k speed of Car K,

P_z position of Car Z which is in the same lane in front of the the ego car,

V_z speed of Car Z,

P_L position of Car L which is same lane behind ego car,

V_L speed of Car L,

P_n position of Car N which is right lane behind the ego car,

V_N speed of Car N,

P_m position of Car M which is right lane in front of the the ego car,

V_k speed of Car M.

Lane change is initiated according to the following rules if Car Ego is in Middle or Right Lane:

- If $V_{ego} \leq V_z$ stay in same lane
- If $V_{ego} > V_z$ then check
    - If $V_{ego} > V_y$ and $V_{ego} \leq V_k$ change to left lane
    - If $V_{ego} < V_y$ and $V_{ego} \leq V_k$ then check
        - Calculate the time Car Y to reach safe distance of Car Ego $T_{Y\_ego\_reach} = \frac{P_{ego} - P_y}{V_{ego} - V_y}$, and calculate the time of Car Ego to takeover Car Z $T_{ego\_z\_to} = \frac{(P_z - P_{ego})}{V_{ego} - V_z}$.
        - $T_{ego\_z\_to} \geq T_{Y\_ego\_reach}$ change the lane to left than pass the Car Z and change to right lane.
        - $T_{ego\_z\_to} < T_{Y\_ego\_reach}$ stay in same lane
    - If $V_{ego} < V_y$ and $V_{ego} \leq V_k$ stay in same lane

Lane change is initiated according to the following rules if Car Ego is in Left Lane:

- If $V_{ego} \leq V_z$ and $V_{ego} > V_L$ stay in same lane
- If $V_{ego} > V_z$ and $V_{ego} > V_L$ check
    - If $V_{ego} > V_n$ and $V_{ego} \leq V_m$ change to right lane
    - If $V_{ego} < V_n$ and $V_{ego} \leq V_m$ and stay in same lane
- If $V_{ego} < V_L$ check
    - If $V_{ego} > V_n$ and $V_{ego} \leq V_m$ change to right lane
    - If $V_{ego} < V_n$ and $V_{ego} \geq V_m$ and stay in same lane
    - If $V_{ego} < V_n$ and $V_{ego} \leq V_m$ and stay in same lane

- Calculate the time Car L to pass the Car Ego

  Ego $T_{L\_ego\_Pass} = \frac{2(P_{ego} - P_l)}{V_L - V_{ego}}$ and calculate the time Car N to reach safe distance to Car ego $T_{n\_ego\_reach} = \frac{(P_{ego} - P_n)}{V_n - V_{ego}}$
- $T_{L\_ego\_Pass} \geq T_{n\_ego\_reach}$ stay in same lane
- $T_{L\_ego\_Pass} < T_{n\_ego\_reach}$ change the lane to right than let the Car L pass and change to left lane.

5.5 Case Studies

In this chapter, we delve into several case studies presenting the application of MPC in various traffic scenarios, integrating insights from the IDM model and other advanced driving systems. These scenarios highlight MPC's effectiveness in enhancing traffic flow, improving safety, and optimizing vehicle behavior under different conditions.

5.5.1 Scenario 1

In the first scenario, a Collision Avoidance System integrated with MPC is tested. The MPC-controlled vehicle dynamically adjusts its speed to close gaps with the vehicle ahead while maintaining a safe distance. This scenario evaluates MPC's ability to react promptly to changes in traffic conditions, demonstrating its potential to enhance safety by preventing rear-end collisions through proactive speed adjustments based on real-time sensor data. Figure 5.6 illustrates the Scenario 1.

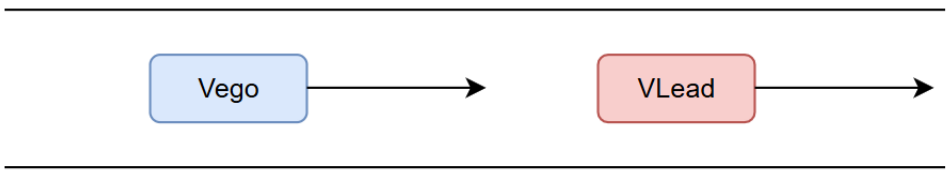

Figure 5.6 Scenario 1

The Figure 5.7 highlights the performance of MPC in avoiding collision with minimal deceleration.

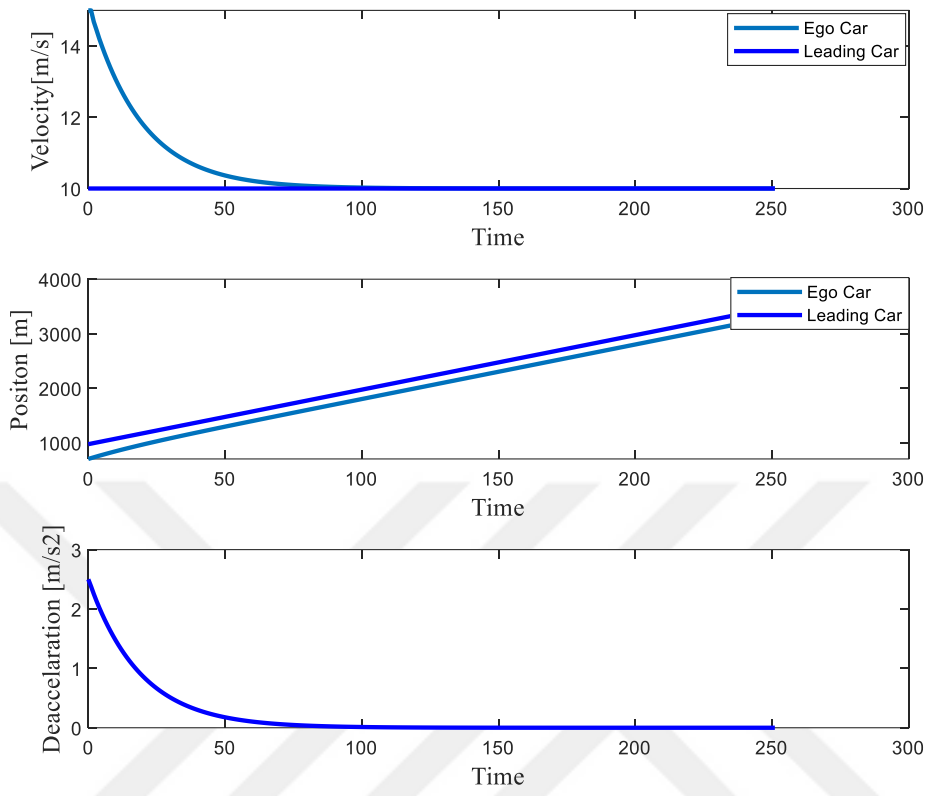

Figure 5.7 Velocity, Position and Deceleration of Scenario 1 Cars

Here, the cars move at 30 km/h (V_{ego}) and 54(V_{Lead}) km/h. Using MPC, a vehicle adjusts the positions of the cars by adjusting deceleration to allow them to maintain a safe distance.

5.5.2 Scenario 2

Scenario 2 focuses on testing a Lane Change Algorithm implemented with MPC. When a neighboring lane is clear, the MPC-controlled vehicle utilizes Lateral PID control to execute lane changes following a predefined Bézier curve setpoint. This scenario assesses MPC's precision in executing lane changes swiftly and smoothly, contributing to smoother traffic transitions and reduced congestion by efficiently utilizing available road space. Scenario 3 is shown in Figure 5.8

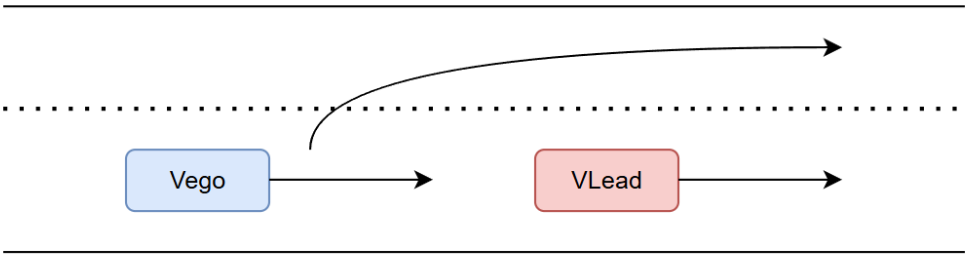

Figure 5.8 Scenario 2

In Figure 5.9, the lane-changing algorithm employs a PID controller with a 7.21% overshoot error to follow a given Bézier curve.

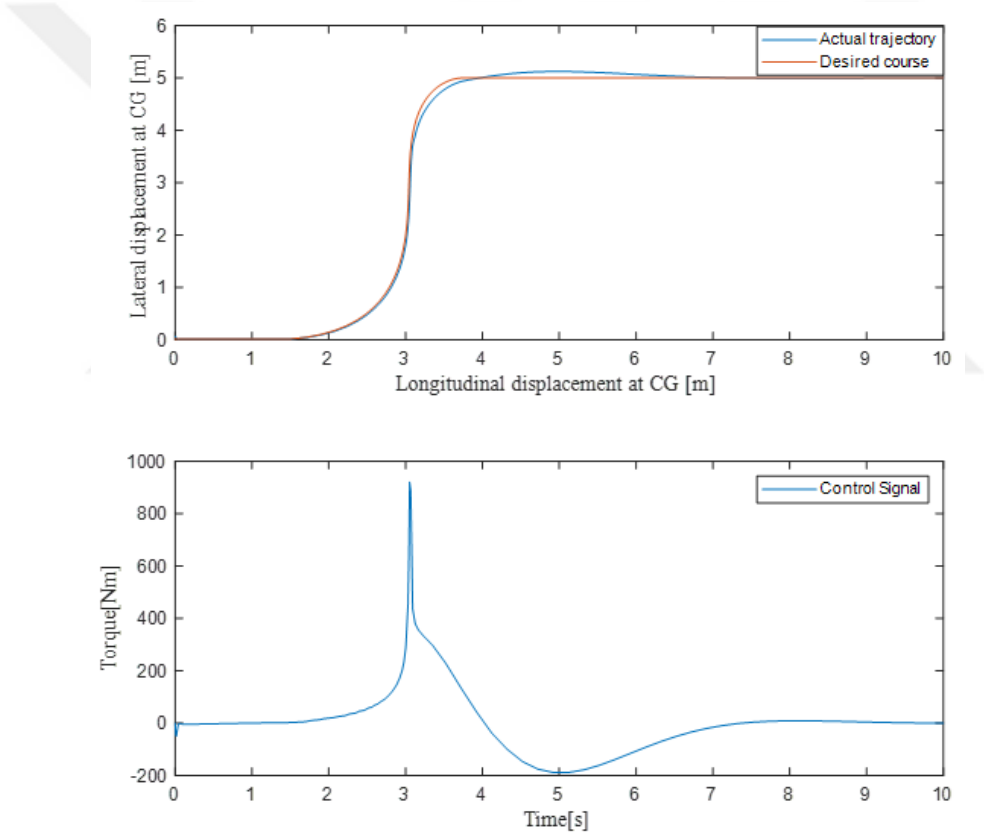

Figure 5.9 Trajectory and Control Signal in Scenario 2

Further tuning of the PID controller could potentially enhance performance. Alternatively, the implementation of more advanced control algorithms, such as LQR (Linear Quadratic Regulator), may offer additional improvements in trajectory tracking and overall system efficiency.

5.5.3 Scenario 3

In the third scenario, which is illustrated in Figure 5.10, the MPC-controlled vehicle faces a situation where the passing time for vehicles in other lanes is significantly prolonged. In response, the MPC system accelerates, executes a lane change to overtake slower vehicles, and returns to its original lane. The trajectories, control signal and speeds of vehicle can be seen in Figure 5.11.

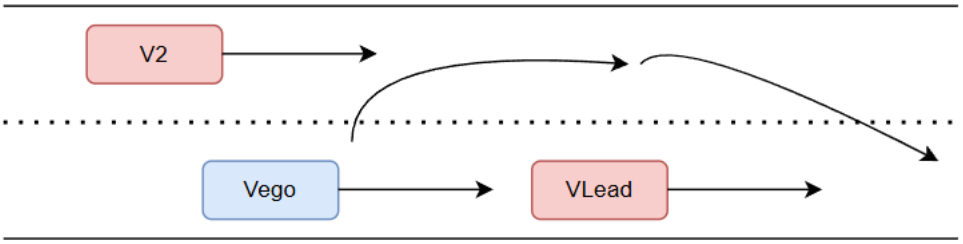

Figure 5.10 Scenario 3

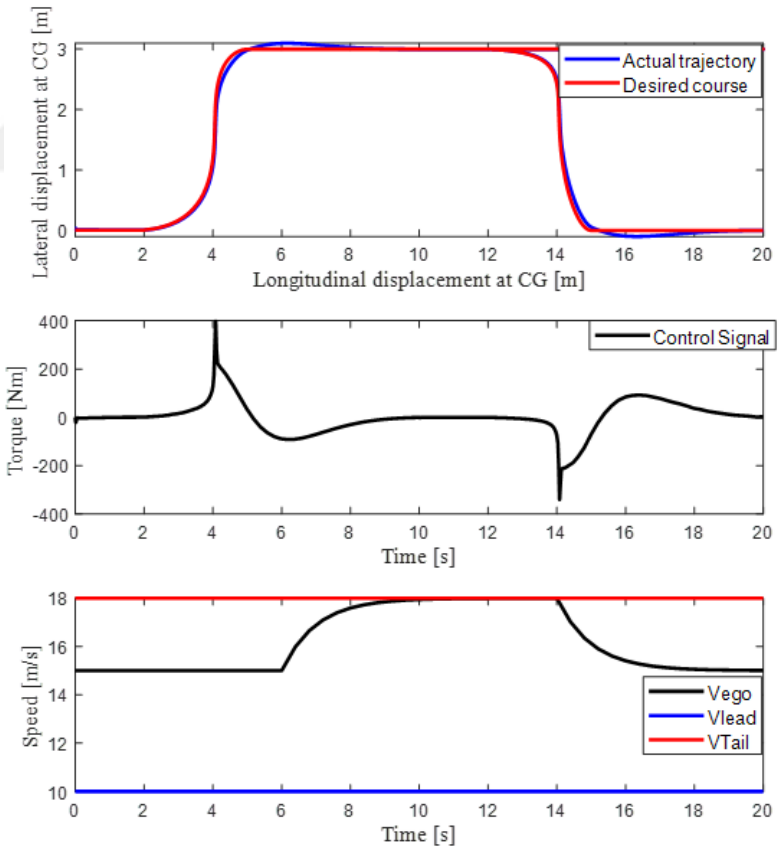

Figure 5.11 Trajectories, Control signal and Speeds of Vehicle in Scenario 3

5.5.4 Scenario 4

The fourth scenario evaluates a Green Wave Control System using MPC against the IDM model across five traffic lights generated from FTP-75 cycle data. Here, each vehicle is tested individually without traffic, aiming to assess the system's ability to optimize the timing of traffic lights for uninterrupted vehicle movement. By comparing MPC's predictive capabilities with IDM's behavioral modeling, the study aims to quantify the effectiveness of MPC in achieving smoother traffic flow and reducing overall travel time. Figure 5.12 show the scenario 4 and position of the vehicles can be seen in Figure 5.13.

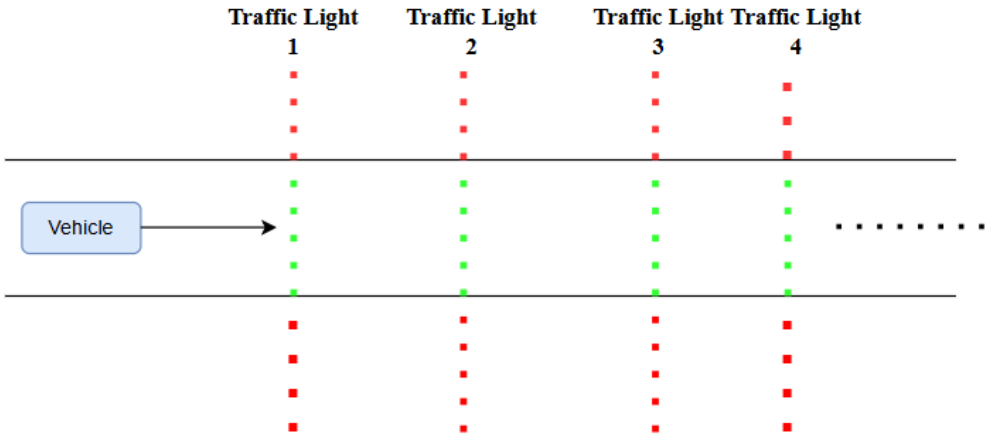

Figure 5.12 Scenario 4

MPC vehicle maintains a relatively smooth acceleration and deceleration, Figure 5.14. However, applying the GWCS algorithm reduces the vehicle’s sudden acceleration and deceleration behaviors. This is because the GWCS algorithm accurately adjusts the desired velocity profile by interacting with traffic signals. Therefore, the GWCS vehicle not only maintains a consistent speed but also improves both energy efficiency

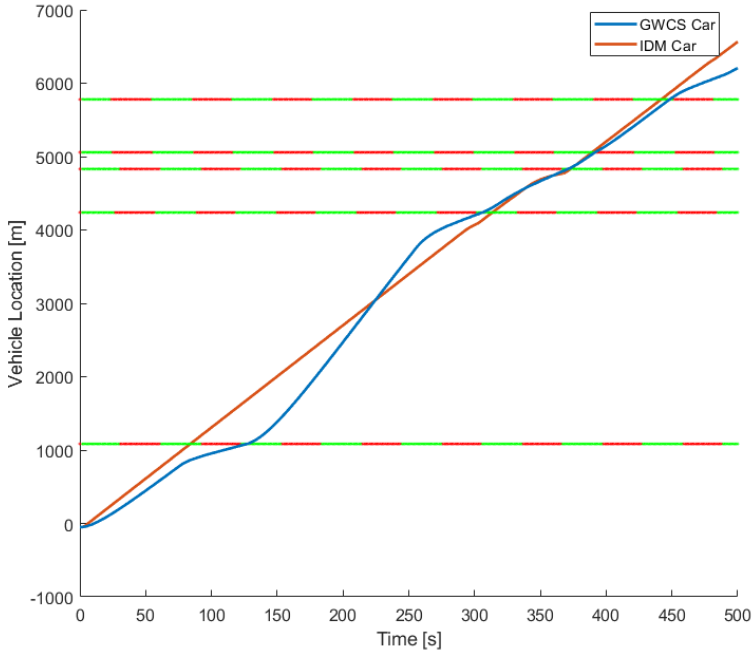

Figure 5.13 Positon of the Vehicles in Scenario 4

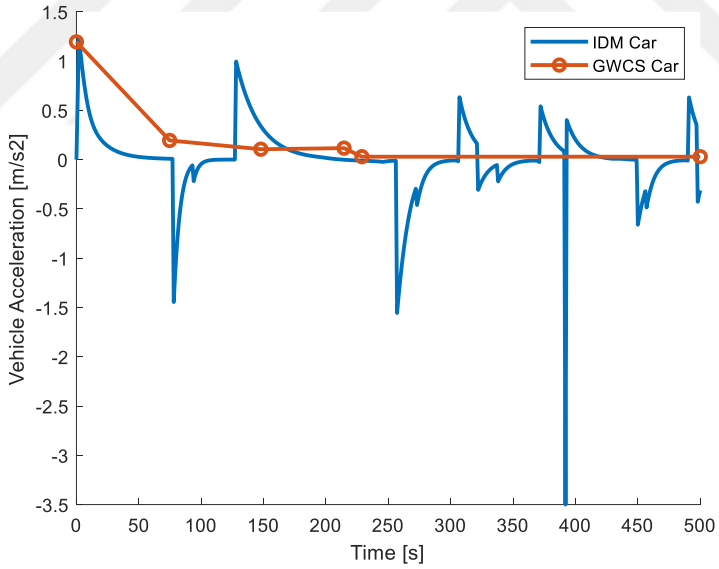

Figure 5.14 Acceleration of Scenario 4 Cars

Table 4.4 Energy Consumption of Vehicles

Vehicle	Energy Consumption (kWh)
GWCS Vehicle	**1.17487 kWh**
IDM Vehicle	**1.824458 kWh**

Table 5.1 presents the energy consumption data for vehicles using the IDM and GWCS. The results clearly indicate that the GWCS vehicle consumes less energy compared to the IDM vehicle. This improved energy efficiency is primarily due to the implementation of the GWCS, which optimizes the vehicle's velocity profile to synchronize with traffic signals.

5.5.5 Scenario 5

The final scenario combines elements from previous scenarios while integrating considerations for energy consumption. The MPC-controlled vehicle follows a predefined speed profile, navigating through lane changes, collision avoidance maneuvers, and overtaking actions as required. This holistic approach not only optimizes traffic flow and safety but also minimizes energy consumption by employing efficient driving strategies tailored to real-time traffic conditions.

In Figure 5.15 the traffic light phases and GWCS, IDM vehicle positions can be seen.

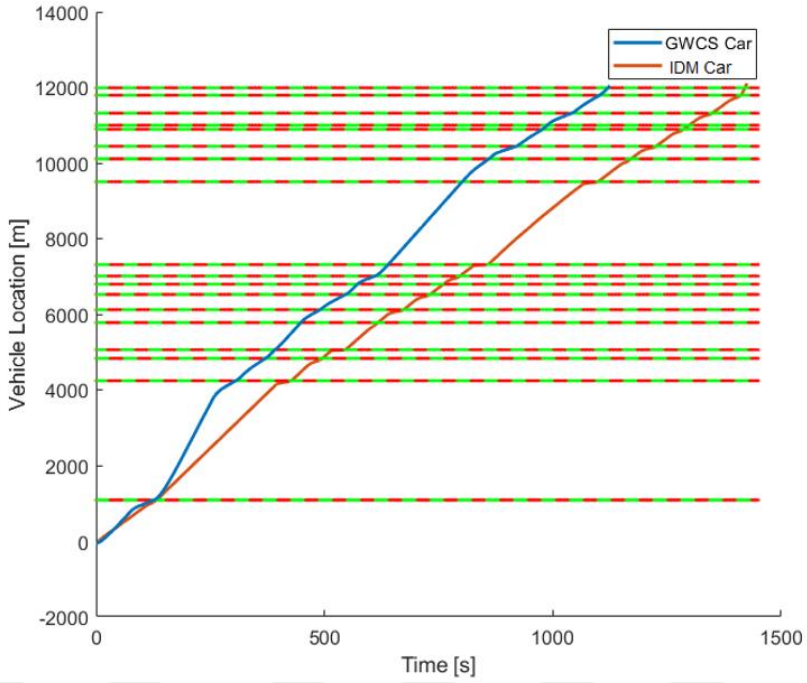

Figure 5.15 Position of the Vehicles and Traffic Light Phases in Scenario 5

The IDM car encountered delays at multiple traffic lights because its primary objective is to reach and maintain its pre-set speed. This behavior results from the IDM's focus on achieving optimal velocity rather than anticipating or reacting proactively to changing traffic conditions. As a result, the car prioritizes acceleration to meet its speed target, which can lead to timing conflicts with red lights or sudden stops, especially in environments with frequent traffic signals. Speeds of GWCS car and IDM car can be seen in Figure 5.16.

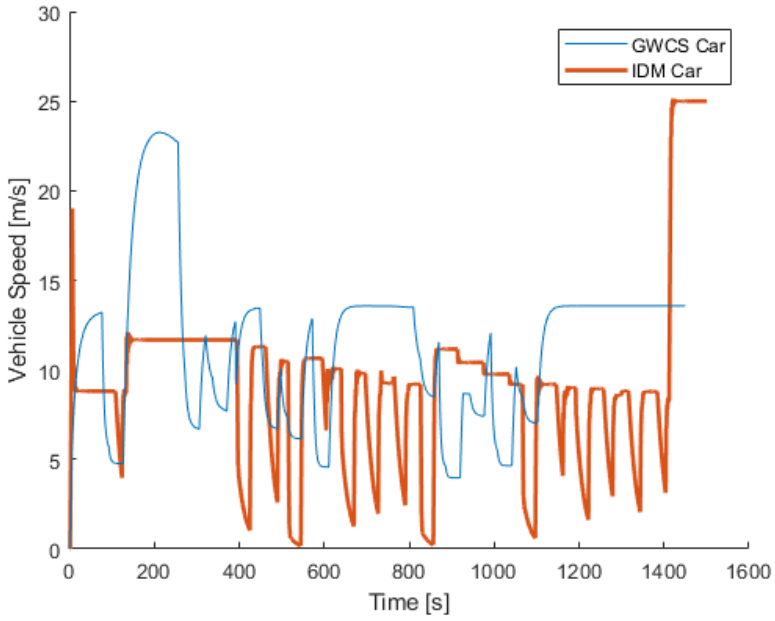

Figure 5.16 Speed of the Vehicles in Scenario 5

To maintain its desired acceleration profile, the GWCS car performed lane changes following a set of pre-defined rules section 5.4. These rules guide the GWCS car's decisions to switch lanes when necessary, ensuring smooth acceleration while adapting to traffic conditions. The lane change information of GWCS car can be seen in Figure 5.17

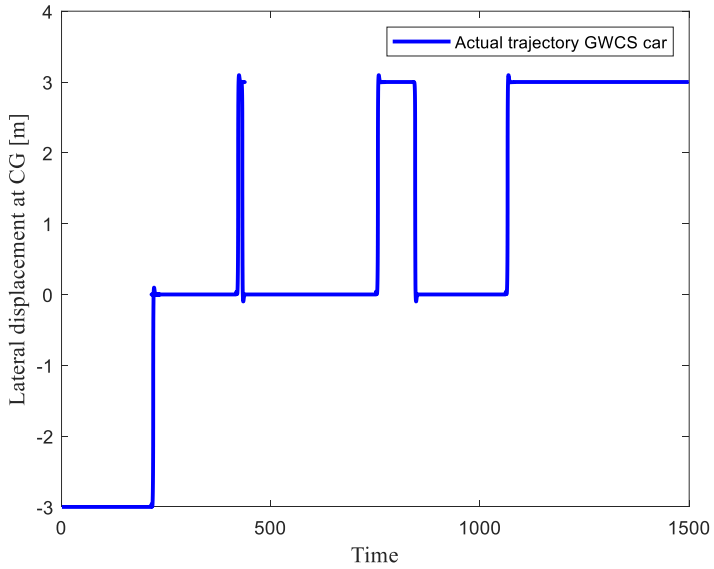

Figure 5.17 Lateral Displacement of GWCS Car in Scenario 5

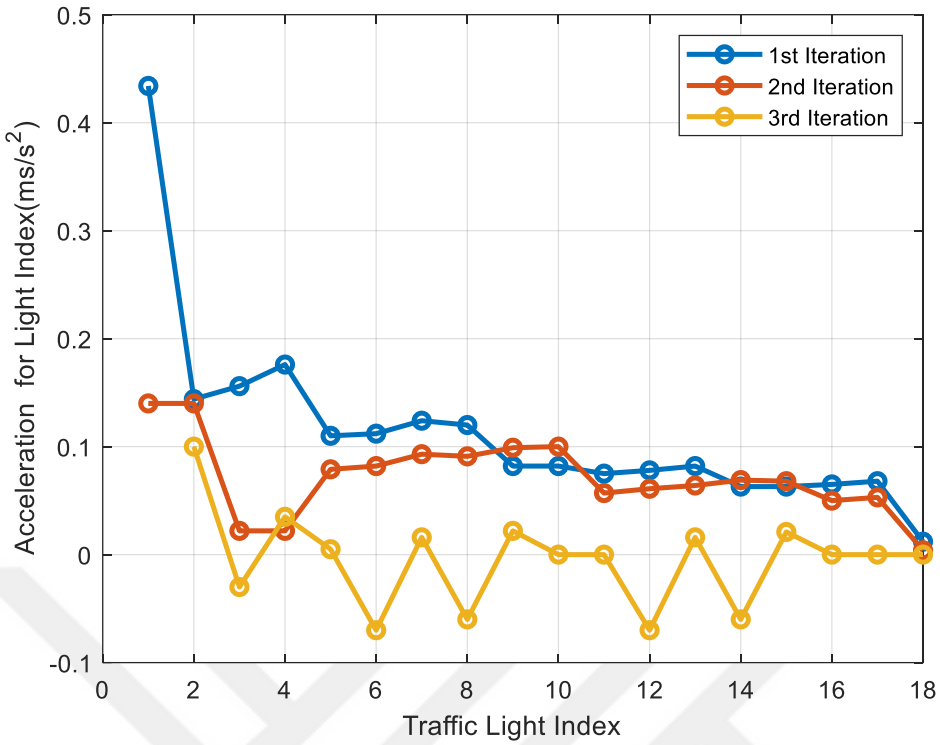

Figure 5.18 Acceleration Setpoints for Light Index

The GWCS algorithm made 3 iterations due to necessary slow-down action in order to avoid collusion. First iteration is done when the simulation started to set the acceleration setpoint profile.

Second iteration is done because the V_{lead} which is the car in front of the GWCS car on the same lane and $V_{leadLeft}$ which is the car in front of the GWCS car on the left lane are stoped at the first traffic light. This scenario is illustrated in Figure 5.18

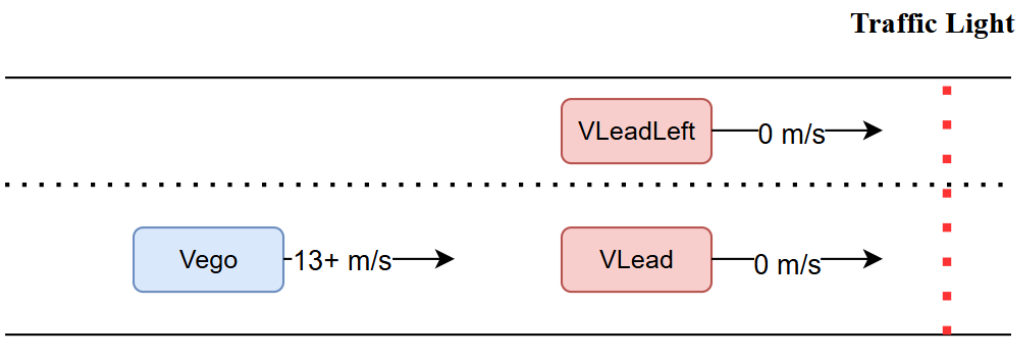

Figure 5.19 Second Iteration Scenario

Since V_{lead} and $V_{leadleft}$ speed are $0\ m/s$ .GWCS car can not change to the left lane. Only option of GWCS car in this scenario is to slow down to avoide collision with V_{lead}. After the traffic light becomes green again V_{lead} and $V_{leadleft}$ increases their speeds to pre-defined set points and the gaps between the GWCS car increases. After this point GWCS algorithm triggered again and calculates the second iteration of acceleration setpoints in Figure 5.18. The speed and position of the V_{lead}, $V_{leadleft}$ and GWCS car can be seen in Figure 5.20.

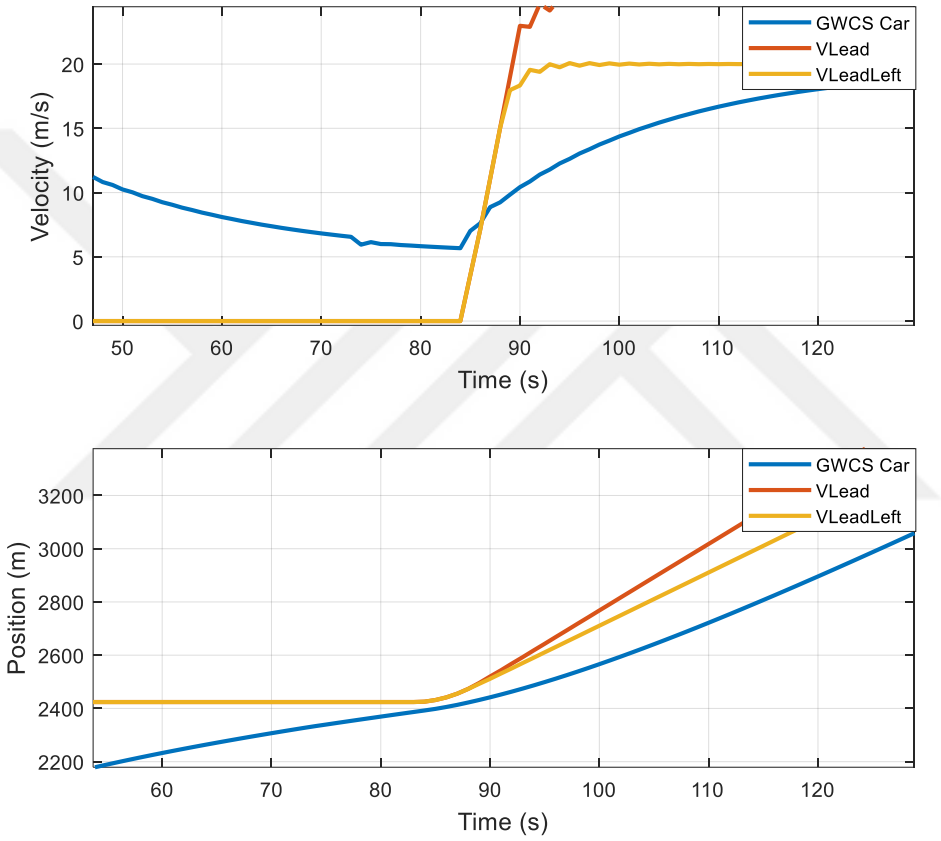

Figure 5.20 Speed and Positions of Iteration 2 of GWCS

Third iteration is done because the V_{lead}, which is the car in front of the GWCS car on the same lane, is slower than GWCS car and $V_{tailLeft}$, which is the car in behind of the GWCS car on the left lane, is faster than GWCS car. This scenario is illustrated in Figure 5.21

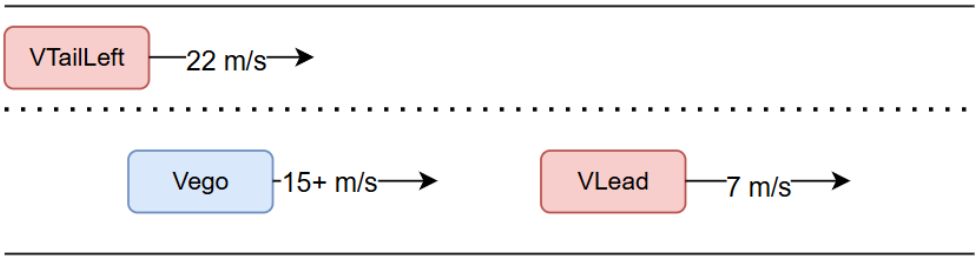

Figure 5.21 Third Iteration Scenario 5

In this scenario, the V_{lead} speed is 7 m/s and $V_{tailLeft}$ speed is 22 m/s while speed of GWCS is 15 m/s and increases with the acceleration setpoint. According to the lane change rules defined in Chapter 5.4. $T_{Tail\_reach} = 5.1\ s$ which is the time of $V_{tailLeft}$ to reach same distance of GWCS car is lower than $T_{GWCS\_Takeover} = 6.04\ s$, which is takeover action time of the GWCS car to V_{lead}. Only option left for GWCS car is slow down to avoid collision and let the $V_{tailLeft}$, then change to left lane. After the lane change GWCS algorithm triggered again and calculates the third iteration of acceleration setpoints in Figure 5.18. The speed and position of the V_{lead}, $V_{tailLeft}$ and GWCS car and lane change information of GWCS car can be seen in Figure 5.22.

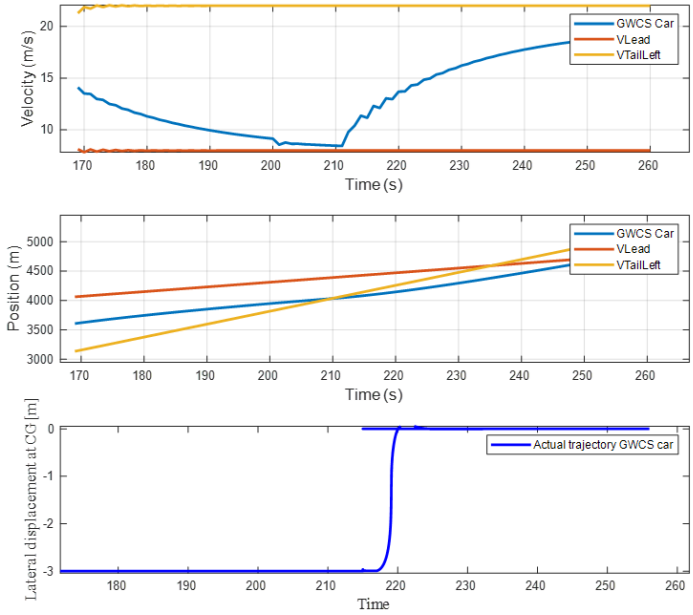

Figure 5.22 Speed, Positions, Lane Information of Iteration 3 of GWCS

Table 4.5 Energy Consumption of Vehicles in FTP 75

Vehicle	Energy Consumption (kWh)
GWCS Vehicle	**9.17487 kWh**
IDM Vehicle	**14.824458 kWh**

Table 5.2 presents the energy consumption data for vehicles using the IDM and GWCS. The results clearly indicate that the GWCS vehicle consumes less energy compared to the IDM vehicle.

In conclusion, these case studies demonstrate the versatility and effectiveness of MPC in enhancing traffic management and vehicle behavior in diverse scenarios. By integrating predictive capabilities with advanced driving algorithms like IDM and collision avoidance systems, MPC proves instrumental in improving safety, reducing congestion, and optimizing energy usage in modern urban environments. These insights pave the way for further advancements in autonomous driving technologies and smarter transportation systems aimed at achieving safer, more efficient mobility solutions

5.5.6 Green Wave Optimization Algorithm Test on Hardware

Testing simulated algorithms on hardware like ECUs (Electronic Control Units) is one of the important steps to validate their real-world performance and reliability. Simulations provide a controlled environment to develop and refine algorithms, but hardware testing ensures these algorithms function correctly under real-world constraints, such as processing power, latency, and environmental variations.

The green wave optimization algorithm is tested on both a simulation computer and in an ECU. The specification of the simulation computer:

- Intel® Raptor Lake Refresh Core™ i9-14900HX 24/32T; 36MB L3; E-CORE Max 4.1 GHZ P-CORE Max 5.8 GHZ;
- 16GB Ram DDR5 5600MHz.

For hardware testing a rapid prototyping ECU from WOODWARD MotoHawk ECM-0565-128-0702C is used. This ECU commonly used for testing prototypes in automotive industry. The speciation of the ECU:

- Microprocessor Freescale MPC565 56Mhz
- 1M Flash 548K Ram 8K Serial EEPROM, 64Kx8 Parallel EEPROM 512K External Ram
- 30 Analog inputs, 8 Digital Inputs, 30 Analog Outputs and 2 Can 2.0B Channels with ISO 9141 compatibility.

Required traffic light information for green wave optimization algorithm to Motohawk ECU and acceleration setpoint from Motohawk ECU is given and taken by CAN signals.

$$CANTL1 = [Latitude, Longitude, First\ Light\ Green\ Time, First\ Light\ Red\ Time \ldots.]$$

Example CAN messages for green wave optimization algorithm inputs.

$$CANMSG = [41.01, 0, 14{:}00{:}42, 14{:}01{:}22 \ldots.]$$

The $Longitude$ of the light are taken as zero since in all simulation the roads are staright lines.

CAN messages are transmitted from a Host PC to ECU and received from ECU to Host PC with the help of a Ksaver Leaf Pro device. The schematic of the hardware test setup can be seen in Figure 5.23.

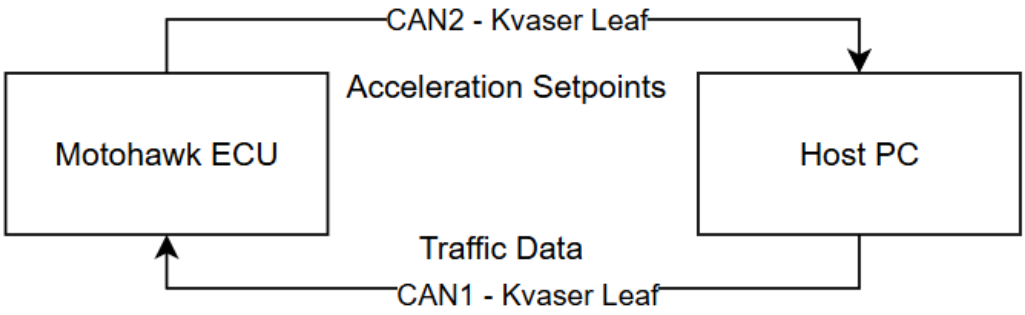

Figure 5.23 Hardware Test Setup

With this setup, the same algorithm ran for same traffic and vehicle conditions. The setpoints calculated from computer simulation and hardware simulation can be seen in Figure 5.24.

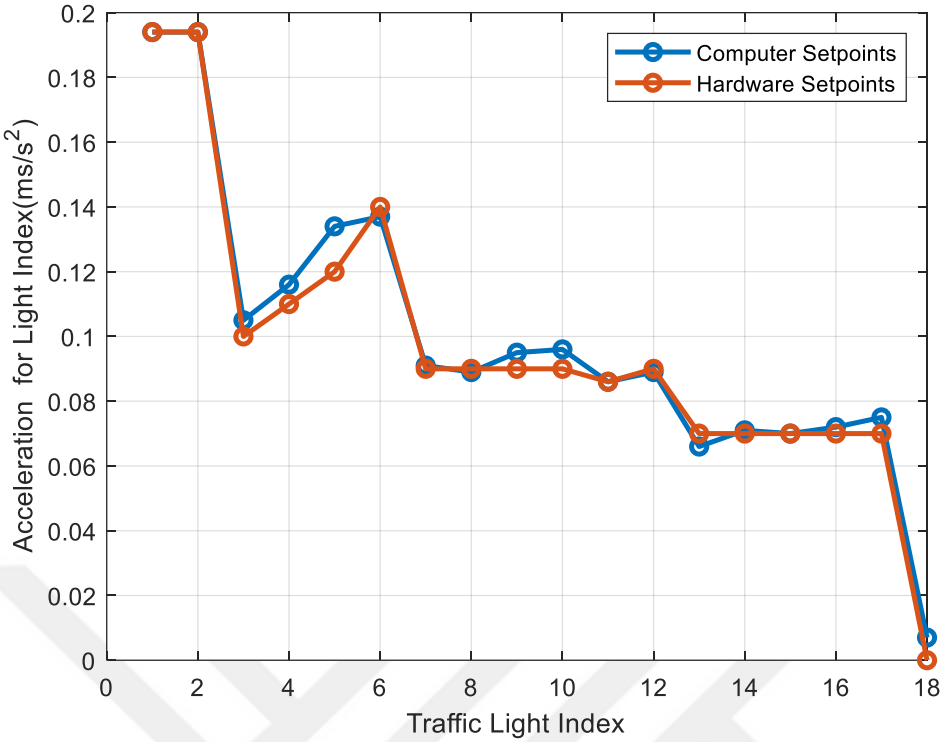

Figure 5.24 Acceleration Setpoint of Computer and Hardware Simulations

The difference between the acceleration setpoint of computer and hardware simulation is caused by the allowed datatype of the Motohawk ECU. In Motohawk ECU only 32-bit signals are allowed but in computer simulation, where we used MATLAB-2023B, 64 bit-double signals are used. The energy cost function can calculate the cost to the 10^{-5}decimal in MATLAB. However, this cannot be achieved in Motohawk ECU.

Table 4.6 Calculation Time of the Green Wave Optimization Algorithm

Simulation Type	**Calculation Time (s)**
Computer Simulation	0.52 s
ECU Simulation	3.17 s

The calculation time of the green wave optimization algorithms can be seen in Table 5.3. Even with the data type simplification of Motohawk ECU the calculation takes more time than the computer simulation. The calculation time of the Motohawk

ECU can be accepted in allowable range to be used in real time scenarios. The maximum calculation time can be added as offset to the current vehicle time to calculate the acceleration setpoint more accurately.

6
CONCLUSION

6.1 Summary of Findings

In conclusion, this thesis study aimed for reducing energy consumption in electric vehicles. Through the integration of a Green Wave control strategy, employing a Neural Network energy model trained with test data, a PID controlled two-wheel lateral model, and an MPC controller for longitudinal dynamics, the approach included careful optimization techniques customized for the Federal Testing Produce Cycle, resulting in very promising outcomes.

Moreover, the proposed controller algorithm was tested against an IDM validating its effectiveness across various scenarios. Specifically, we evaluated the GWCS, collision avoidance system by MPC, and a lane change algorithm integrating Bézier curves.

The outcomes of our various scenarios are promising. We observed a notable decrease in energy usage, resulting in an approximate 30% improvement. Additionally, our collision avoidance system effectively prevented potential accidents, and the lane change algorithm performed well with only a 7% overshoot. These successes demonstrate the effectiveness of our approach in improving energy efficiency.

By testing our algorithm on hardware, we can demonstrate its applicability for real-world applications. Simulated environments are useful for initial development and validation, but they cannot fully replicate the complexities of physical systems. Hardware testing, such as on ECUs, allows us to verify that the algorithm performs as intended under real-world constraints.

6.2 Contributions to the Field

The findings from the study underscore the potential of model predictive control in achieving optimal energy consumption and improving the sustainability of electric vehicles. The green wave control strategy has demonstrated significant fuel savings, further enhancing the overall sustainability and cost-effectiveness of electric

vehicles. By providing a seamless and efficient driving experience while optimizing energy consumption, this strategy represents a significant advancement in the field of green vehicle technology.

6.3 Recommendations for Future Research

Moving forward, our focus lies on implementing more efficient optimization algorithms for (GWCS). We plan to rigorously test these algorithms across a spectrum of scenarios to ensure their robustness and adaptability. Furthermore, we intend to validate their effectiveness by conducting extensive experiments using real-world traffic data, providing a comprehensive assessment of their performance under diverse conditions.

REFERENCES

[1] A Research and US DOT or DOT) Innovative Technology Administration (RITA) United States Department of Transportation (USDOT. Vehicle-to-vehicle(v2v)communicationsforsafety.http://www.its.dot.gov/research/v2v.htm, 2014.

[2] Research and US DOT or DOT) Innovative Technology Administration (RITA) United States Department of Transportation (USDOT. Vehicle-to-infrastructure(v2i)communicationsforsafety.http://www.its.dot.gov/research/v2i.htm, 2014.

[3] Lakshmi, G. S., Rubanenko, O., & Hunko, I. (2020). Renewable Energy Generation and Impacts on E-Mobility. In G. S. Lakshmi, O. Rubanenko, & I. Hunko, Journal of Physics Conference Series (Vol. 1457, Issue 1, p. 12009). IOP Publishing. https://doi.org/10.1088/1742-6596/1457/1/012009

[4] Kumbaroğlu, G., Canaz, C., Deason, J. P., & Shittu, E. (2020). Profitable Decarbonization through E-Mobility. In G. Kumbaroğlu, C. Canaz, J. P. Deason, & E. Shittu, Energies (Vol. 13, Issue 16, p. 4042). Multidisciplinary Digital Publishing Institute. https://doi.org/10.3390/en13164042

[5] Rajnoha, R., Jankovský, M., & Merková, M. (2014). Economic Comparison of Automobiles with Electric and with Combustion Engines: An Analytical Study. In R. Rajnoha, M. Jankovský, & M. Merková, Procedia - Social and Behavioral Sciences (Vol. 109, p. 225). Elsevier BV. https://doi.org/10.1016/j.sbspro.2013.12.449

[6] Soltani-Sobh, A., Heaslip, K., Stevanović, A., Bosworth, R., & Radivojevic, D. (2017). Analysis of the Electric Vehicles Adoption over the United States. In A. Soltani-Sobh, K. Heaslip, A. Stevanović, R. Bosworth, & D. Radivojevic, Transportation research procedia (Vol. 22, p. 203). Elsevier BV. https://doi.org/10.1016/j.trpro.2017.03.027

[7] Ramachandaramurthy, V. K., Ajmal, A. M., Kasinathan, P., Tan, K. M., Yong, J. Y., & Vinoth, R. (2023). Social Acceptance and Preference of EV Users—A Review. In V. K. Ramachandaramurthy, A. M. Ajmal, P. Kasinathan, K. M. Tan, J. Y. Yong, & R. Vinoth, IEEE Access (Vol. 11, p. 11956). Institute of Electrical and Electronics Engineers. https://doi.org/10.1109/access.2023.3241636

[8] Liu, Y., Yao, C., Guo, C., Yang, Z., & Fu, C. (2023). Energy-Saving Optimization for Electric Vehicles in Car-Following Scenarios Based on Model Predictive Control. World Electric Vehicle Journal, 14(2), 42. https://doi.org/10.3390/wevj14020042

[9] Tang, K., Lv, H., Zhong, X., Xu, T., Guo, T. (2024). Path-Oriented Green Wave Speed Control Model Towards Autonomous Vehicle. In: Qu, Y., Gu, M., Niu, Y., Fu, W. (eds) Proceedings of 3rd 2023 International Conference on Autonomous Unmanned Systems (3rd ICAUS 2023). ICAUS 2023. Lecture Notes in Electrical Engineering, vol 1177. Springer, Singapore. https://doi.org/10.1007/978-981-97-1103-1_10

[10] A. Liu, C. Li, B. Xia, W. Yue and Z. Miao, "G-MACO: A Multi-Objective Route Planning Algorithm on Green Wave Effect for Electric Vehicles," 2018 IEEE 87th Vehicular Technology Conference (VTC Spring), Porto, Portugal, 2018, pp. 1-5, doi: 10.1109/VTCSpring.2018.8417768.

[11] Wang, Jinwen & Gao, Xiujing & Duan, Huijie & Liu, Xin & Huang, Hongwu. (2022). Study of vehicle-road cooperative green wave traffic strategy for traffic signal intersections. 187-192. 10.1109/ICEDCS57360.2022.00048.

[12] P. Huang, C. Li, Q. Luo, Y. Zhang and B. Xia, "GECM: A Novel Green Wave Band Based Energy Consumption Model for Electric Vehicles," 2018 IEEE 87th Vehicular Technology Conference (VTC Spring), Porto, Portugal, 2018, pp. 1-5, doi: 10.1109/VTCSpring.2018.8417767.

[13] M.A.S. Kamal, J. Imura, A. Ohata, T. Hayakawa, and K. Aihara, "Control of Traffic Signals in a Model Predictive Control Framework," in Proceedings of the 2012 IFAC Conference on Control of Traffic Signals, pp. 225-226, September 12-14, 2012, Sofia, Bulgaria

[14] Kural, E., Jones, S., Parrilla, A. F., & Grauers, A. (2014). Traffic Light Assistant System for Optimized Energy Consumption in an Electric Vehicle. AVL Powertrain Engineering, AVL GmbH, Graz, Austria & Chalmers University of Technology, Göteborg, Sweden.

[15] Konstantinos Katsaros, Ralf Kernchen, Mehrdad Dianati, and David Rieck. Performance study of a green light optimized speed advisory (glosa) application using an integrated cooperative its simulation platform. In Wireless Communications and Mobile Computing Conference (IWCMC), 2011 7th International, pages 918–923. IEEE, 2011.

[16] Ramon Souza Schwartz, Martijn van Eenennaam, Georgios Karagiannis, Geert Heijenk, Wouter Klein Wolterink, and Hans Scholten. Using v2v communication to create over-the-horizon awareness in multiple-lane highway scenarios. In Intelligent Vehicles Symposium (IV), 2010 IEEE, pages 998–1005. IEEE, 2010.

[17] Behrang Asadi and Ardalan Vahidi, "Predictive Use of Traffic Signal State for Fuel Saving," in IEEE Transactions on Intelligent Transportation Systems, vol. 11, no. 3, pp. 143-153, 2009

[18] Zhong, D., Sun, P., & Boukerche, A. (2020). Empirical Study and Analysis of the Impact of Traffic Flow Control at Road Intersections on Vehicle Energy Consumption. In 18th ACM International Symposium on Mobility Management and Wireless Access (MobiWac'20), November 16–20, 2020, Alicante, Spain. ACM

[19] Wang, L., Pan, K., & Wang, X. (2017). Real-time Queue Length Perception with Green Wave Band Point Optimization Based on Floating Vehicle. 2017 IEEE 6th Data Driven Control and Learning Systems Conference

[20] Nicholas J. Kohut, J. Karl Hedrick, and Francesco Borrelli, "Integrating Traffic Data and Model Predictive Control to Improve Fuel Economy," Mechanical Engineering Department, University of California-Berkeley, Berkeley, CA, USA.

[21] J. Yan, P. Shao, Q. Chen, M. Zhang, Z. Li, and L. Wang, "A Study of Bidirectional Green Wave Control Based on Random Optimal Graphical Method," DDCLS'18, Beijing, 2018, pp. 1-5.

[22] L. Tan, W. Zhang, and F. Zhang, "Research on Energy Efficiency System of New Energy Vehicle Electric Drive," in IOP Conf. Series: Earth and Environmental Science, vol. 223, 2019,

[23] Y. Shi, J. Li, Q. Han, and L. Lv, "A Coordination Algorithm for Signalized Multi-Intersection to Maximize Green Wave Band in V2X Network," in IEEE Access, vol. 8, pp. 213717-213726, 2020

[24] F. Qiao, X. Tan, and F. A. Tobi, "Optimization of bidirectional green wave of traffic systems on urban arterial road," presented at the 9th International Conference on Modelling, Identification and Control (ICMIC 2017), Kunming, China, July 10-12, 2017.

[25] Engin Ozatay, Umit Ozguner, Dimitar Filev, and John Michelini. Analytical and numerical solutions for energy minimization of road vehicles with the existence of multiple traffic lights. In Decision and Control (CDC), 2013 IEEE 52nd Annual Conference on, pages 7137–7142. IEEE, 2013.

[26] Kobayashi, Takao, et al. "Direct yaw moment control and power consumption of in-wheel motor vehicle in steady-state turning." Vehicle System Dynamics 55.1 (2017): 104-120.

[27] Raksincharoensak, Pongsathorn, Masao Nagai, and Motoki Shino. "Lane keeping control strategy with direct yaw moment control input by considering dynamics of electric vehicle." Vehicle System Dynamics 44.sup1 (2006): 192-201.

[28] MATLAB. (2023). MATLAB Optimization Toolbox. The MathWorks, Inc.

[29] Ho, Yi-Ju, and Jing-Sin Liu. "Collision-free curvature-bounded smooth path planning using composite Bezier curve based on Voronoi diagram." *2009 IEEE International Symposium on Computational Intelligence in Robotics and Automation-(CIRA)*. IEEE, 2009.

[30] Elhoseny, Mohamed, Alaa Tharwat, and Aboul Ella Hassanien. "Bezier curve based path planning in a dynamic field using modified genetic algorithm." *Journal of Computational Science* 25 (2018): 339-350.

[31] Li, Hongluo, Yutao Luo, and Jie Wu. "Collision-free path planning for intelligent vehicles based on Bézier curve." IEEE Access 7 (2019): 123334-123340.

[32] Ü. Özgüner, "Role of Controlin Autonomous Systems" in Autonomous Ground Vehicles, Springer, 2011, pp. 32-36.

[33] Treiber, M., Hennecke, A., & Helbing, D. (2000). Congested Traffic States in Empirical Observations and Microscopic Simulations. *ArXiv*. https://doi.org/10.1103/PhysRevE.62.1805

[34] Elhoseny, Mohamed, Alaa Tharwat, and Aboul Ella Hassanien. "Bezier curve based path planning in a dynamic field using modified genetic algorithm." *Journal of Computational Science* 25 (2018): 339-350.

[35] Li, Hongluo, Yutao Luo, and Jie Wu. "Collision-free path planning for intelligent vehicles based on Bézier curve." IEEE Access 7 (2019): 123334-123340.

[36] Ü. Özgüner, "Role of Controlin Autonomous Systems" in Autonomous Ground Vehicles, Springer, 2011, pp. 32-36.

[37] Treiber, M., Hennecke, A., & Helbing, D. (2000). Congested Traffic States in Empirical Observations and Microscopic Simulations. *ArXiv*. https://doi.org/10.1103/PhysRevE.62.1805

[38] Amijos, A. S. C., Li, A., Cassandras, C. G., Al-Nadawi, Y. K., Araki, H., Chalaki, B., Moradi-Pari, E., Mahjoub, H. N., & Tadiparthi, V. (2022). Cooperative Energy and Time-Optimal Lane Change Maneuvers with Minimal Highway Traffic Disruption. In A. S. C. Armijos, A. Li, C. G. Cassandras, Y. K. Al-Nadawi, H. Araki, B. Chalaki, E. Moradi-Pari, H. N. Mahjoub, & V. Tadiparthi, arXiv (Cornell University). Cornell University. https://doi.org/10.48550/arxiv.2211.08636

[39] Kornbluth, K., Burke, A., Wardle, G., & Nickell, N. (2004). Design of a Freeway-Capable Narrow Lane Vehicle. In K. Kornbluth, A. Burke, G. Wardle, & N. Nickell, SAE technical papers on CD-ROM/SAE technical paper series. https://doi.org/10.4271/2004-01-0760

[40] Eichelberger, A. H., & McCartt, A. T. (2013). Volvo Drivers' Experiences With Advanced Crash Avoidance and Related Technologies. In A. H. Eichelberger & A. T. McCartt, Traffic Injury Prevention (Vol. 15, Issue 2, p. 187). Taylor & Francis. https://doi.org/10.1080/15389588.2013.798409

[41] Coskun, S. (2021). Autonomous overtaking in highways: A receding horizon trajectory generator with embedded safety feature. In S. Coskun, Engineering Science and Technology an International Journal (Vol. 24, Issue 5, p. 1049). Elsevier BV. https://doi.org/10.1016/j.jestch.2021.02.005

APPENDIX A

A.1 Parameter of Vehicle Table

Parameter	Value
m [kg]	1500
Te [Nm]	520
η	0
N	0
r_w[m]	0.36
$Af[m^2]$	2.77
Cd	0.29
I [kg.m^2]	300
Cf [N/m]	12000
Cr [N/m]	16000
lf [m]	0.85
lr [m]	0.75

PUBLICATIONS FROM THE THESIS

Conference Papers

1. F. Ozkan, M. S. Arslan and H. Mercan, "Green Wave Control Strategy for Optimal Energy Consumption by Model Predictive Control in Electric Vehicles," *2024 International Congress on Human-Computer Interaction, Optimization and Robotic Applications (HORA)*, Istanbul, Turkiye, 2024, pp. 1-8, doi: 10.1109/HORA61326.2024.10550469.